Index

North Sea FLOW Measurement Workshop

# Paper 8.1

# Gas Densitometer Applied for Simple Method in Standard Density Determination – Approach to CO2-Emmission Factor Determination for Fuel Gas

*Maron Dahlström*
*StatoilHydro ASA*

TÜV SÜD

nel technology for life

# Gas Densitometer Applied for Simple Method in Standard Density Determination – Approach to CO2-Emmission Factor Determination for Fuel Gas

**Maron J. Dahlström, StatoilHydro ASA**

## 1 INTRODUCTION

From the start of Snorre B, the use of the available fuel gas from Snorre B became a challenge. This gas has a very high MW equal to 36, and is therefore required at a high temperature ( 120 degree C ), to insure gas phase.

Since a Peek densitometer was available, Steinar Fosse suggested that equations could be developed from the density and flowing condition. The need for Standard Density was obvious. Rough correction was applied since the fuel gas system start in July 2001.

However, the precise method for compensation was introduced in 2006, following a NPD audit

Where Steinar Fosse suggested that a more correct method using the available densitometer information, could be applied

## 2 DEVELOPMENT OF STANDARD DENSITY RELATION

Around 1980, I did find that compensations could be closely estimated for a differential device from a densitometer flowing density reading: This method required that the
flow computer used a start composition for density ( AGA8 ) and standard density ( ISO 6976).

The quantities from the flow computer could then be corrected :

Correct Mass = Flowcompter Mass * SQRT ( Densitometer / Density Calc )
as well known, and then standard volume could be calculated, using a very constant A :

Comp Std Vol = Flowcomputer Std Vol * ( A * (Density calc / **Densitometer** -1) + 1 )

And thus; Standard Density = Std Dens Calc * SQRT ( Densitometer / Density Calc ) /
( A * (Density calc / **Densitometer** -1) + 1 )

Standard Density = Standard Density calculated from simulated composition *

SQRT ( Densitometer/ AGA8 Density calc ) / ( A * (Density calc / **Densitometer** -1) + 1 )

However the constant A could vary somewhat with the flowing conditions at Snorre B and the varying gas composition.

### 2.1 Compensated Standard Density

Because of the many difficulties to deal with high MW gas, neither by Gas Chromatography or by sampling methods – a gas densitometer was introduced for Snorre B Fuel Gas in the design phase before 1999.

In the first period of operation in 2001, it was used mainly as a guide to indicate how close we were to the real standard volume, which the NPD regulations did require. Because of the strongly varying composition, the 1980ies method could not be applied directly. However with A = E / Used Standard Dens, we were ready to modify the manual compensations for NPD.

In 2006 the method was verified with simulated composition available from the design shown in Table 1 and Table 2. With a potentially very high MW and with significant variation, an automatic online approach with standard density calculated every 10 second period, was found practical and was then applied in June 2007 with the improved correlation found to better match a wider range of gasses, used with A = E / Standard Density from the composition used in the flow computer.

Using : A = E / ISO6976 Standard Density calculated from simulated initial composition

Compensated Standard Density =ISO6976 Standard Density *SQRT ( Dcalc /**Densitometer** )/
(A * (Dcalc / **Densitometer** -1)+1)

where Dcalc is Density calculated with AGA8 from the initial start composition.

| | | |
|---|---|---|
| $q_m$ | Mass Flow Rate | Kg/h |
| $Cq_m$ | Compensated Mass Flow Rate | Kg/h |
| $Q_m$ | Mass Total | Kg |
| $CQ_m$ | Compensated Mass Total | Kg |
| $q_{std}$ | Standard Volume Flow Rate | $Sm^3/h$ |
| $Cq_{std}$ | Compensated Standard Volume Flow Rate | $Sm^3/h$ |
| $Q_{std}$ | Standard Volume Total | $Sm^3$ |
| $CQ_{std}$ | Compensated Standard Volume Total | $Sm^3$ |
| $\rho_{std}$ | Standard Density ISO 6976 (1995) | $Kg/Sm^3$ |
| $C\rho_{std}$ | Compensated Standard Density | $Kg/Sm^3$ |
| $\rho$ | Density AGA8 (1994) | $Kg/m^3$ |
| $\rho_{meas}$ | Measured Densitometer Density | $Kg/m^3$ |
| E | Pre-determined Compensation Constant – set to | 0,370 |
| $CQ_{m\ corr}$ | Compensated Mass Correction Value | Kg |
| $CQ_{std\ corr}$ | Compensated Standard Volume Correction Value | $Sm^3$ |

1. **Compensated Mass Flow Rate**

$$Cq_m = q_m * \ SQRT\ (\rho_{meas} / \rho)$$

2. **Compensated Mass Flow Total**

$$CQ_m = Q_m * \ SQRT\ (\rho_{meas} / \rho)$$

3. **Compensated Standard Volume Flow Rate**

$$Cq_{std} = q_{std} * (1 + E / \rho_{std} * (\rho / \rho_{meas} - 1 ) )$$

4. **Compensated Standard Volume Total**

$$CQ_{std} = Q_{std} * (1 + E / \rho_{std} * (\rho / \rho_{meas} - 1 ) )$$

5. **Compensated Standard Density**

$$C\rho_{std} = Q_m / Q_{std} * SQRT\ (\rho_{meas} / \rho) / (1 + E / \rho_{std} * (\rho / \rho_{meas} - 1 ) )$$

**Table 1 - Match based on Compensation with Simulated Composition Start**

| E= 0,370 | 110 degC, 32 BarA | 115 degC, 34 BarA | 120 degC, 36 Bar | 125 degC, 38 BarA |
|---|---|---|---|---|
| Flow computer Density | 43,27738 | 45,480945 | 47,60596 | 49,652902 |
| Flow computerr Standard Density | 1,54458 | 1,54458 | 1,54458 | 1,54458 |
| | | | | |
| Case1 Measured Dens | 40,249207 | 42,286977 | 44,25517 | 46,154415 |
| Case 1 Standard Density | **1,475034** | **1,475034** | **1,475034** | **1,475034** |
| Flowcom Dens/ Measured Dens | 1,075235594 | 1,075530772 | 1,073957870 | 1,075799617 |
| Compensated Standard Density | **1,472715** | **1,472411** | **1,472221** | **1,472135** |
| Bias % | + 0,16 | + 0,18 | + 0,19 | + 0,20 |
| | | | | |
| Case 2 Measured Dens | 38,711437 | 40,665985 | 42,555261 | 44,379951 |
| Case 2 Standard Density | **1,433317** | **1,433317** | **1,433317** | **1,433317** |
| Flowcom Dens/ Measured Dens | 1,117948166 | 1,11840264 | 1,118685628 | 1,118813809 |
| Compensated Standard Density | **1,430025** | **1,429584** | **1,429309** | **1,429185** |
| Bias % | - 0,23 | + 0,26 | - 0,28 | - 0,29 |
| | | | | |
| Case 3 Measured Dens | 41,987524 | 44,120027 | 46,177749 | 48,161245 |
| Case 3 Standard Density | **1,520353** | **1,520353** | **1,520353** | **1,520353** |
| Flowcom Dens/ Measured Dens | 1,030719982 | 1,030845811 | 1,030928554 | 1,030972144 |
| Compensated Standard Density | **1,5200003** | **1,519866** | **1,519775** | **1,519727** |
| Bias % | - 0,02 | - 0,03 | - 0,03 | - 0,04 |
| | | | | |

In a close examination, standard density calculations was performed with ISO 6976, ( f995 ) and density calculations was performed with AGA8 , (1994 ), to create simulated density values from densitometer – as well as initial standard density and density at the expected variety of flowing temperature and temperature conditions.

To insure the compensation for correct Standard Density, the indication was that the composition used for the initial density and standard density calculations, need to be sufficiently close to the real composition. However, the tolerance for MW variations would still allow a rather reasonable wide variation of gas compositions

For a period up front before the system was taken into use, low MW gas ( MW 24,6) was still being used for fuel gas, due to temporary limitation in the compressor turbine. See table 2 for verification of the compensation method. This was the gas used in almost all of 2006.

This was back to normal ( MW 36 )in July 2007. The initial gas composition in the flow computer was then soon changed to better match the gas used for fuel. This gas was used mainly to avoid having to flare high MW gas from Snorre B. The possibility to export the heavier components to Snorre A , was not an option at that time.

This examination showed that Standard density could be controlled for prediction of standard density with acceptable tolerance (expected +/- 0,5 %) in spite of the varying conditions, also with the expected variation of composition. The dependence of the starting gas composition in the flow computer was checked for final compensated results. This examination was made as a table of expected conditions and a mix of the available simulated gas compositions, covering expected gasses..

**Table 2 - Match based on Compensation with Simulated Composition Start**

| E= 0,370 | 110 degC, 32 BarA | 115 degC, 34 BarA | 120 degC, 36 Bar | 125 degC, 38 BarA |
|---|---|---|---|---|
| Flow computer Density | 26,167537 | 27,452373 | 28,698848 | 29,90793 |
| Flow computerr Standard Density | 1,045057 | 1,045057 | 1,045057 | 1,045057 |
| | | | | |
| Case1 Measured Dens | 25,950066 | 27,223702 | 28,45949 | 29,658313 |
| Case 1 Standard Density | 1,037483 | 1,037483, | 1,037483 | 1,037483 |
| Flowcom Dens/ Measured Dens | 1,008380364 | 1,008399703 | 1,008410481 | 1,008419826 |
| Compensated Standard Density | **1,037637** | **1,037561** | **1,033491** | **1,037602** |
| Bias % | + 0,01 | + 0,01 | + 0,02 | + 0,01 |
| | | | | |
| Case 2 Measured Dens | 31,904244 | 33,491117 | 35,0285316 | 36,517416 |
| Case 2 Standard Density | **1,23245** | **1,23245** | **1,23245** | **1,23245** |
| Flowcom Dens/ Measured Dens | 0,820189847 | 0,819691174 | 0,819299202 | 0,819004554 |
| Compensated Standard Density | **1,232406** | **1,233013** | **1,239474** | **1,233850** |
| Bias % | - 0,00 | + 0,05 | + 0,08 | + 0,11 |
| | | | | |
| Case 3 Measured Dens | 25,438149 | 26,686306 | 27,837413 | 29,072425 |
| Case 3 Standard Density | **1,018877** | **1,018877** | **1,018877** | **1,018877** |
| Flowcom Dens/ Measured Dens | 1,0228672998 | 1,028706371 | 1,030945225 | 1,028738745 |
| Compensated Standard Density | **1,020044** | **1,020016** | **1,018109** | **1,019988** |
| Bias % | + 0,13 | + 0,11 | - 0,08 | + 0,11 |

The check indicated that the method would generate acceptable compensation over a wide range, providing that the used composition in the flow computer is adjusted when the composition changes significantly.

The nature of operation limit the variations over a short span of time. For the last year, the maximum long term changer is limited to 6 % below the composition used. The less significant short term changes has been limited to +/- 22 %, still generating answers well inside +/- 1 % after compensation.

The EU CO2-emmission directive was adopted by the Norwegian Pollution Board. who also requested that real life samples should be collected for accredited analysis – in order to verify the method used ,with an uncertainty budget of +/- 1,5 % for volume and mass, and +/- 0,5 % for the CO2-Emission Factor With the Peek densitometer calibration uncertainty of +/- 0,3 % and similar +/-0,3 % for the temperature the effect correction from 20 degC to 120 DegC, only +/-0,3 % was available for the computer calculation of standard density, in addition to the +/- 0,37 % effect carried from the densitometer into the standard density calculation This was possible to keep under control by changing the start composition, to stay within the required uncertainty.

**Table 3 - Match based on Compensation with Sample Composition Start**

| **E= 0,370** | 110 degC, 32 BarA | 115 degC, 34 BarA | 120 degC, 36 Bar | 125 degC, 38 BarA |
|---|---|---|---|---|
| Flow computer Density | 4196408 | 44,083863 | 46,139324 | 48,120718 |
| Flow computerr Standard Density | **1,52042** | **1,52042** | **1,52042** | **1,52042** |
| | | | | |
| Case1 Measured Dens | 39,691319 | 41,692862 | 43,62610 | 45,49177 |
| Case 1 Standard Density | **1,46220** | **1,46220** | **1,46220** | **1,46220** |
| Flowcom Dens/ Measured Dens | 1,057260808 | 1,057350369 | 1,057608267 | 1,05776953 |
| Compensated Standard Density | **1,458353** | **1,458260** | **1,457991** | 1,457803 |
| Bias % | -0,26 | - 0,27 | - 0,29 | - 0,30 |
| | | | | |
| Case 2 Measured Dens | 43, | 45,487347 | 47,12294 | 49,49177 |
| Case 2 Standard Density | **1,55446** | **1,556114** | **1,556114** | **1,556114** |
| Flowcom Dens/ Measured Dens | 0,96950913 | 0,969147816 | 0,979126599 | 0,969019956 |
| Compensated Standard Density | **1,555687** | **1,56114** | **1,544386** | **1,556266** |
| Bias % | + 0,08 | + 0,11 | > | + 0,12 |
| | | | | |
| Case 3 Measured Dens | 38,842005 | 40,976726 | 42,685361 | 44,508608 |
| Case 3 Standard Density | **1,43940** | **1,43940** | **1,43940** | **1,43940** |
| Flowcom Dens/ Measured Dens | 1,089378832 | 1,075829313 | 1,080916804 | 1,081153127 |
| Compensated Standard Density | **1,434705** | **1,439298** | **1,434164** | **1,433926** |
| Bias % | -0,33 | - 0,01 | -0,37 | -0,38 |

The many attempts to collect gas samples showed as expected that heavier component would be lost from the MW 36 gas, as was expected when the method was developed.

Taking samples at the high MW and high temperature, can not be done. The samples taken was found at MW 29 to 32. At this high MW, gas chromatographs would also require very high temperatutre to present close to correct results.

The first attempts showed how difficult it was to achieve correct samples. With the MW 36 gas ; as low as MW 29 was found. So the Argon backpressure was focused, together with minimum isolation against severe temperature exchange.

**Table 4 - Match based on Compensation with Sampled Composition verified**

| **E= 0,370** | 110 degC, 32 BarA | 115 degC, 34 BarA | 120 degC, 36 Bar | 125 degC, 38 BarA |
|---|---|---|---|---|
| Flow computer Density | 36,842005 | 40,976726 | 42,685361 | 44,508698 |
| Flow computerr Standard Density | **1,43940** | **1,43940** | **1,43940** | **1,43940** |
| | | | | |
| Case1 Measured Dens | 32,173403 | 33,77329 | 35,323258 | 36,82423 |
| Case 1 Standard Density | **1,24238** | **1,24238** | **1,24238** | **1,24238** |
| Flowcom Dens/ Measured Dens | 1,2072706 | 1,213287956 | 1,208420837 | 1,208679666 |
| Compensated Standard Density | **1,243757** | **1,238850** | **1,242816** | **1,242605** |
| Bias % | + 0,11 | - 0,28 | + 0,04 | + 0,02 |
| | | | | |
| Case 2 Measured Dens | 35,082155 | 36,837196 | 38,535873 | 40,179047 |
| Case 2 Standard Density | **1,33149** | **1,33149** | **1,33149** | **1,33149** |
| Flowcom Dens/ Measured Dens | 1,107172721 | 1,112373645 | 1,107678578 | 1,107758927 |
| Compensated Standard Density | **1,331286** | **1,326444** | **1,330813** | **1,330738** |
| Bias % | - 0,02 | + 0,38 | - 0,05 | - 0,06 |
| | | | | |
| Case 3 Measured Dens | 41,96408 | 44,083963 | 46,139324 | 48,120718 |
| Case 3 Standard Density | **1,52042** | **1,52042** | **1,52042** | **1,52042** |
| Flowcom Dens/ Measured Dens | 0,925601252 | 0,929516479 | 0,925140581 | 0,92493836 |
| Compensated Standard Density | **1,525301** | **1,520526** | **1,525865** | **1,526113** |
| Bias % | +0,32 | + 0,01 | + 0,36 | +0,37 |

The high MW needed to be collected at high temperature without significant Joule Thompson pressure loss and good isolation against temperature loss, in order to avoid loosing the heavier components,

The samples therefore had to be regarded as partial composition only. In table 4 it was checked that these compositions could be verified against the compensation method, in preparation for lower MW fuel gas options.

Using the possibilities to change the start composition in the flow computer, more accurate standard volume and mass results could be controlled within tight limits, by changing the starting composition for the flow computer more frequently. The sampled composition was also checked as a start to flow computer calculations, and verified to accurate compensations. In table 5.

**Table 5 - Match based on Compensation with Sampled Composition Start**

| E= 0,370 | 110 degC, 32 BarA | 115 degC, 34 BarA | 120 degC, 36 Bar | 125 degC, 38 BarA |
|---|---|---|---|---|
| Flow computer Density | 32,587726 | 34,846294 | 35,78325 | 37,305884 |
| Flow computer Standard Density | **1,25436** | **1,25436** | **1,25436** | **1,25436** |
| | | | | |
| Case1 Measured Dens | 36,054594 | 37,863696 | 39,614177 | 41,306846 |
| Case 1 Standard Density | **1,35880** | **1,35880** | **1,35880** | **1,35880** |
| Flowcom Dens/ Measured Dens | 0,903643987 | 0,903527722 | 0,903294004 | 0,903135621 |
| Compensated Standard Density | **1,357812** | **1,358280** | **1,358552** | **1,358736** |
| Bias % | - 0,03 | - 0,04 | -0,02 | 0.00 |
| | | | | |
| Case 2 Measured Dens | 28,905436 | 30,22606 | 31,603392 | 32,938418 |
| Case 2 Standard Density | **1,13506** | **1,13506** | **1,13506** | **1,13506** |
| Flowcom Dens/ Measured Dens | 1,1313048 | 1,131834549 | 1,13225979 | 1,13258821 |
| Compensated Standard Density | **1,135349** | **1,34912** | **1,134562** | **1,134291** |
| Bias % | + 0,03 | - 0,01 | - 0,04 | - 0,07 |
| | | | | |
| Case 3 Measured Dens | 35,0821155 | 36,837196 | 38,535873 | 40,179047 |
| Case 3 Standard Density | **1,33149** | **1,33149** | **1,33149** | **1,33149** |
| Flowcom Dens/ Measured Dens | 0,928897555 | 0,92897012 | 0,928569855 | 0,928486034 |
| Compensated Standard Density | **1,32149** | **1,329578** | **1,329729** | **1,329823** |
| Bias % | - 0,16 | - 0,14 | - 0,13 | - 0,13 |

Without the compensation method, there was no chance to achieve the requirements in the EU CO2-emmission Directive. The remaining uncertainty would the be as high as +/- 11 %. However when applying the compensation method, both standard volume and mass could be available within +/- 0,9 % uncertainty.

Standard density was well within +/- 0,5 %. ( 0,5 % from densitometer will result in +/- 0,37 % plus some minor uncertainties like +/- 0,03 % from ISO 6967 and +/- 0,10 % from AGA8. For compensated standard density, adding the +/- 0,3 % allowed for compensation standard density calculations., we still are well inside the EU requirement of +/- 0,5 %.

**CO2- Emission Factor to be within +/- 0,50 %**

The samples taken for SFT in June 2008, contained gas from MW 32,7 to MW 33,7. So it was decided to make a last attempt, ensuring that the fuel gas really was stable and as high as wanted for the high MW composition point needed: Above MW 36 was confirmed for all samples taken, and proper Argon backpressure was used. Still the results were from MW 29,1 to MW 31,2. No insulation against temperature loss was applied, so the real fuel gas composition could not be sampled correctly:. Therefore it was decided to compute the CO2-Emmissioi Factor by mixing the simulated composition of MW 35,7 with the different partial samples found in June and August, to arrive at the average compensated standard density determined for June, July and August- presented in table 7.

**Table 7 – CO2_Emmission Factor**

| Month | Avg: Std Dens Kg/Sm3 | Mix1 % | Mix 2 % | CO2- Factor |
|---|---|---|---|---|
| June 2008 | **1,45785** | 64,940 %<br>1,42463 | 36,060 %<br>1,51955 | Kg CO2/Sm3<br>**4.2669** |
| June 2008 | 1,45785 | 48,25 %<br>1,39188 | 51,75 %<br>1,51955 | Kg CO2/Sm3<br>**4.2689** |
| June 2008 | 1,45785 | 32,700<br>1,33149 | 57,300<br>1,51955 | Kg CO2/Sm3<br>**4.2632** |
| June 2008 | 1,45785 | 22,34%<br>1,2438 | 77,66 %<br>1,51955 | Kg CO2/Sm3<br>**4.2646** |
| | | | | |
| July 2008 | **1,44212** | 81,240 %<br>1,42463 | 18,460 %<br>1,51955 | Kg CO2/Sm3<br>**4.2156** |
| July 2008 | 1,44212 | 39,430 %<br>1,39188 | 60,570 %<br>1,51955 | Kg CO2/Sm3<br>**4.2181** |
| July 2008 | 1,44212 | 41,055 %<br>1,33149 | 58,945<br>1,51955 | Kg CO2/Sm3<br>**4,2109** |
| July 2008 | 1,44212 | 27,795 %<br>1,2438 | 72,205 %<br>1,51955 | Kg CO2/Sm3<br>**4,2127** |
| | | | | |
| August 2008 | **1,45440** | 68,58 %<br>1,42463 | 31,42 %<br>1,51955 | Kg CO2/Sm3<br>**4.2557** |
| August 2008 | 1,45440 | 50,95 %<br>1,39188 | 49,05 %<br>1,51955 | Kg CO2/Sm3<br>**4,2578** |
| August 2008 | 1,45440 | 34,532 %<br>1,33149 | 65,488<br>1,51955 | Kg CO2/Sm3<br>**4,2517** |
| August 2008 | 1,45440 | 23,38 %<br>1,24238 | 76,62 %<br>1,51955 | Kg CO2/Sm3<br>**4,2532** |

The table 7 review, with the CO2-Emission Factor calculation, which result in maximum difference all inside +/- 0,10 %, indicates that the CO2- Emission Factor can be determined with this method ; well within the EU CO2-Emmission Directive requirement of +/_ 0,50 %.

This suggests that this method can also be used for other fuel stations, where the gas composition vary too much for manual sampling, or where the operating temperature make other instrumentation options troublesome. At this moment also Snorre A is considered as a good candidate, with operation around 70 degrees C and MW varying between 22,2 to 22,8.

North Sea FLOW Measurement Workshop

# Paper 8.2

# Handbook Of Uncertainty Calculations – Ultrasonic Fiscal Oil Metering Stations


***Per Lunde***
***University of Bergen***

***Kjell-Eivind Frøysa***
***Christian Michelsen Research AS (CMR)***

***Svein Neumann***
***Norwegian Society for Oil and Gas Measurement (NFOGM) and ConocoPhillips***

***Steinar Vervik***
***Norwegian Petroleum Directorate (NPD)***


TÜV SÜD

nel technology for life

# Handbook of Uncertainty Calculations – Ultrasonic Fiscal Oil Metering Stations

**Per Lunde, University of Bergen**
**Kjell-Eivind Frøysa' Christian Michelsen Research AS (CMR)**
**Svein Neumann, Norwegian Society for Oil and Gas Measurement (NFOGM) and ConocoPhillips**
**Steinar Vervik, Norwegian Petroleum Directorate (NPD)**

## ABSTRACT

A "*Handbook of uncertainty calculations - Ultrasonic fiscal oil metering stations"* [1] is being developed in a cooperation between NFOGM, NPD, Tekna and CMR, addressing fiscal metering of oil using multipath ultrasonic transit time flow meters (USM). The many different approaches to calculating the uncertainty of ultrasonic oil metering stations have been a source of confusion; - varying practice in this respect has definitely been experienced. The intention of the present initiative has been that a handbook together with a spreadsheet program *EMU - USM Fiscal Oil Metering Stations*, based upon the principles laid down in the "*Guide to the expression of uncertainty in measurement (GUM)"* [2] and ISO 5168:2005 [3], would satisfy the need for a modern method of uncertainty evaluation in the field of ultrasonic fiscal oil measurement.

Three different metering station scenarios are being addressed in [1]: (a) Scenario A, a USM "duty meter" which is *in-situ* calibrated using a prover; (b) Scenario B, a USM "duty meter" which is operated together with a USM "master meter", which is *in-situ* calibrated using a prover; and (c) Scenario C, a USM "duty meter" which is operated together with a turbine (TM) "master meter", which is *in-situ* calibrated using a prover.

The present paper gives a description of Scenario A. Calculation of the expanded uncertainties of the following three metering station measurands are addressed: the actual volumetric flow rate, the standard volumetric flow rate and the mass flow rate. The analytical uncertainty model accounts for metering station instrumentation such as pressure transmitter, temperature element and transmitter, density measurement (vibrating element densitometer), prover and a multipath ultrasonic gas flow meter (USM). The expanded uncertainty of each of these measurands and instruments can be calculated and analyzed, isolated and combined (for the metering station). The basis for the *Handbook* and the program is described, together with an illustration example of a metering station uncertainty evaluation.

## 1 INTRODUCTION

### 1.1 Uncertainty evaluation of ultrasonic fiscal metering stations

Regulations relating to fiscal measurement of oil and gas [4-6] require that the overall measurement uncertainty is documented to be within defined limits. However, the different methods used have given different results. Consistent and standardised methods of uncertainty evaluation have been required, so that different measurement systems could be directly and reliably compared.

On this background, a series of handbooks on uncertainty calculation of fiscal metering stations for oil and gas is being developed in a cooperation between the Norwegian Society for Oil and Gas Measurement (NFOGM), the Norwegian Petroleum Directorate (NPD), Tekna and Christian Michelsen Research (CMR). This series includes handbooks of uncertainty calculations for ultrasonic fiscal gas metering stations [8,9] and for fiscal orifice gas and turbine oil metering stations [10]. The series is being extended by a handbook of uncertainty calculations for ultrasonic fiscal oil metering stations [1]. These handbooks are developed in conformity with the ISO "*Guide to the expression of uncertainty in measurement"* (commonly

referred to as the *"Guide*" or the "*GUM"*) [2], which provides general rules for evaluating and expressing uncertainty in measurement, intended for a broad scope of measurement areas.

### 1.2 The *Handbook*

The *Handbook of uncertainty calculations - USM fiscal oil metering stations* [1] (for convenience here referred to as the *"Handbook")* consists of the *Handbook* itself and the Microsoft Excel program *EMU - USM Fiscal Oil Metering Stations* for performing uncertainty calculations of fiscal oil metering stations based on multipath ultrasonic transit time flow meters (USM), and individual instruments of such stations (cf. Section 2).

The USM fiscal oil metering stations addressed in the *Handbook* are primarily taken to be built and operated according to NPD regulations [4]. For USM fiscal metering of oil, the NPD regulations refer to e.g. the NORSOK I-105 national standard [5] and the API standard on ultrasonic liquid hydrocarbon meters [6] as recognised standards ("accepted norms"). The NPD regulations require hydrocarbon metering stations to be in conformity with the requirements stated by the European Union's "measurement instrument directive" (MID) [7]. Both the NPD regulations and the NORSOK I-105 standard refer to the *GUM* [2] as the "accepted norm" with respect to uncertainty analysis.

The *Handbook* and the accompanying computer program *EMU - USM Fiscal Oil Metering Stations* are based primarily on the recommended procedures in the *GUM*, in conformity with ISO 5168:2005 [3] (also based on the *GUM*).

With respect to uncertainty evaluation and documentation, refs. [3,4] state that the expanded uncertainty of the metering station shall be specified at a 95 % confidence level, using a coverage factor $k = 2$. Consequently, for output expanded uncertainties $k = 2$ is set as a fixed value in the program. For input expanded uncertainties, however, $k$ is set by the user for each input uncertainty value (depending on the confidence level of the input uncertainty in question).

The uncertainty model for the USM oil metering station used here is based on an analytical approach. That is, the uncertainty models involving the USM, prover, pressure transmitter, temperature element/transmitter, densitometer, etc., are fully analytical, with expressions given and documented for the model and the sensitivity coefficients. The model is treated at a sufficiently generic level so that all relevant USM types for oil measurement are covered (cf. e.g. [11-14]), irrespective of path configuration, including non-reflecting path as well as reflecting path USMs. The intention has been to meet as far as possible manufacturer data specified today with respect to instrument uncertainties, including the USM. The work builds on earlier developments in this field [15-19,8-10].

The *Handbook* [1] is intended to provide a practical approach to the field of uncertainty calculations of ultrasonic fiscal oil metering stations. It is primarily written for experienced users and operators of fiscal oil metering stations, manufacturers of ultrasonic oil flow meters, engineering personnel as well as others with interests within the field. It has been the intention that the Excel program may be run without needing to read much of the *Handbook*, such as the theory part. However, Chapter 5 in the *Handbook* which gives an overview of the program, as well as Chapter 4 which - through an uncertainty evaluation example - provides some guidelines for specifying input parameters and uncertainties to the program, may be useful to read together with running the program for the first time.

## 2 USM FISCAL OIL METERING STATIONS

The types of fiscal oil metering stations considered in the *Handbook* consist basically of a USM "duty meter" ($q_v$), a prover, in some applications a "master meter" (which may be a USM or a turbine meter (TM)), a flow computer, and instrumentation such as pressure transmitter ($P$), temperature element and transmitter ($T$), and vibrating element densitometer ($\rho$).

Table 1. Characteristics for the 3 scenarios A, B and C of the types of USM fiscal oil metering stations addressed in the *Handbook*.

| Operational scenario | Instrumentation for flow calibration and proving |
|---|---|
| Scenario A | A USM ”duty meter” which is *in-situ* calibrated using a prover, typically every 4th day. |
| Scenario B | A USM ”duty meter” which is operated together with a USM ”master meter”.<br>The USM ”duty meter” is *in-situ* calibrated vs. the USM ”master meter”.<br>The USM ”master meter” is *in-situ* calibrated vs. a prover, typically once a year. |
| Scenario C | A USM ”duty meter” which is operated together with a turbine (TM) ”master meter”.<br>The USM ”duty meter” is *in-situ* calibrated vs. the TM ”master meter”.<br>The TM ”master meter” is *in-situ* calibrated vs. a prover, typically once a year. |

With respect to flow calibration and proving of the USM "duty meter" and the "master meter" (USM or TM), three different operational scenarios A, B and C are considered in the *Handbook* [1], cf. Table 1.

In the present paper, Scenario A only is addressed in the following. For this case, consider a fiscal oil metering station equipped with instrumentation as specified in Table 2.

Table 2. Equipment specified as default instrumentation for ***Scenario A*** of the USM fiscal oil metering station addressed in the *Handbook*. Included is also example instrumentation used for uncertainty evaluation of a fiscal oil metering station in Section 5.

| Measurement | Instrument |
|---|---|
| Ultrasonic "duty meter" (USM) | Multipath ultrasonic transit time flow meter. Otherwise not specified.<br>*In-situ* calibrated by use of prover, typically every 4th day. |
| Prover | Not specified (arbitrary). |
| Flow computer | Not specified (arbitrary). |
| Pressure (static), *P* | Not specified.<br>Example: Rosemount 3051P Reference Class Pressure Transmitter [20]. |
| Temperature, *T* | Not specified.<br>Example: Pt 100 element: according to EN 60751 tolerance A [5].<br>Rosemount 3144 Smart Temperature Transmitter [21]. |
| Density, $\rho$ | On-line (by-pass) installed vibrating element densitometer. Otherwise not specified.<br>Example: Solartron 7835 Liquid Density Transducer [22]. |

For fiscal oil metering stations, three flow rates are in question [5]:

- Actual volumetric flow rate (i.e. the axial volumetric flow rate at line conditions), $q_v$,
- Standard volumetric flow rate (i.e., the axial volumetric flow rate at standard reference conditions), $Q_v$, and
- Mass flow rate, $q_m$.

For Scenario A, these are given as[1] [1]

$$q_v = 3600 \cdot C_{prov} \cdot q_{USM} \qquad [\mathrm{m^3/h}] , \qquad (1a)$$

$$Q_v = \frac{\rho}{\rho_{ref}} q_v = q_v \cdot C_{tlm} \cdot C_{plm} \qquad [\mathrm{Sm^3/h}] , \qquad (1b)$$

$$q_m = \rho q_v = \rho_{ref} Q_v = \frac{\rho_d}{C_{tld} \cdot C_{pld}} Q_v \qquad [\mathrm{kg/h}] , \qquad (1c)$$

respectively. The "proving correction factor"

$$C_{prov} \equiv f_{prov}(C_1^{prov}, C_2^{prov}, ..., C_M^{prov}) \qquad (2)$$

is some function, $f_{prov}$, of the *M* meter factors,

[1] Symbols are defined at the end of the paper.

$$C_j^{prov} = \frac{K_{DFC}}{K_{prov,j}^{USM}}, \qquad j = 1, \ldots, M, \tag{3}$$

where the meter factors $C_j^{prov}$ are calculated from the K-factors, $K_{prov,j}^{USM}$, $j$ = 1, …, $M$, which are obtained by proving of the USM at $M$ different nominal test flow rates ("proving points") [1]. The DFC (digital-to-frequency converter) factor $K_{DFC}$ is used to let the USM deliver pulses per second as its output quantity, and is specified by the USM manufacturer [1].

Typically, $M$ is 4 to 6, and $C_{prov}$ may be flow rate dependent. Methods for calculation of the correction factor $C_{prov}$ from the $M$ meter factors $C_j^{prov}$ (cf. Eq. (2)) include various types of single-factor and multi-factor corrections[2]. The uncertainty model described here covers any of these methods. In fact, for use of the uncertainty program one does not need to know $C_{prov}$ nor the method used for calculating $C_{prov}$. It is sufficient to know the corrected relative deviation after $C_{prov}$ has been applied, $Dev_{C,j}$, defined by Eq. (9).

The functional relationships of the USM, pressure transmitter, temperature element/transmitter and liquid densitometer, which form the basis for the uncertainty model described in Section 3, are described in [1]. Due to space limitations these are not given here.

## 3 UNCERTAINTY MODEL OF THE OIL METERING STATION

For the three measurands given in Eqs. (1), the relative combined standard uncertainties are given as [1]

$$E_{q_v}^2 = E_{proving}^2 + E_{USM}^2 + E_{comm}^2 + E_{flocom}^2, \tag{4a}$$

$$E_{Q_v}^2 = E_{q_v}^2 + E_{C_{tlm}}^2 + E_{C_{plm}}^2 + correlation\ terms\ A, \tag{4b}$$

$$E_{q_m}^2 = E_{Q_v}^2 + E_{\rho d}^2 + E_{C_{tld}}^2 + E_{C_{pld}}^2 + correlation\ terms\ B, \tag{4c}$$

respectively. In Eqs. (4), "correlation terms A" refer to correlations between the volume correction factors $C_{tlm}$, $C_{plm}$ and the volume correction factors $C_{tlp}$, $C_{plp}$, $C_{tsp}$ and $C_{psp}$ appearing in Eqs. (1b) and (1a), respectively (cf. also Eq. (10)). Furthermore, "correlation terms B" refer to correlations between the volume correction factors $C_{tld}$, $C_{pld}$ and the above mentioned volume correction factors. Such correlations are neglected in the simplified calculation example given here, cf. Section 5.

The corresponding relative expanded uncertainties at a 95 % confidence level are obtained by multiplying with the coverage factor $k$ = 2 (assuming a normal probability distribution).

The derivation underlying the uncertainty model given by Eqs. (4) is rather comprehensive, and for details it is referred to [1]. The model has been obtained by a detailed analysis of correlated and uncorrelated effects in the USM, such as for the USM in duty operation vs. proving, between the various acoustic paths of the USM, between upstream and downstream signal propagation in a given acoustic path (correlated and uncorrelated transit time contributions), etc. Thus, elimination of systematic effects in the USM by proving is accounted for, so that these do not contribute to the metering station uncertainty. The analysis is made in compliance with the procedure for evaluating and expressing

[2] Single-factor correction methods for calculation of the "proving correction factor" $C_{prov}$ include e.g. (a) the flow-weighted mean error (FWME) [23], (b) the weighted mean error (WME) [24], and average meter factor methods. Multi-factor correction methods include e.g. (a) piecewise linear interpolation [23], (b) multi-point (higher order) polynomial algorithms [23], and (c) regression analysis methods.

uncertainties recommended in [2][3]. The various terms involved in Eqs. (4) are further described in the following.

### 3.1 Pressure transmitter uncertainty

The relative combined standard uncertainty of the pressure measurement is given as $E_P \equiv u_c(\hat{P})/\hat{P}$, where [1,10]

$$\begin{aligned} u_c^2(\hat{P}) = {} & u^2(\hat{P}_{transmitter}) + u^2(\hat{P}_{stability}) + u^2(\hat{P}_{RFI}) + u^2(\hat{P}_{temp}) \\ & + u^2(\hat{P}_{atm}) + u^2(\hat{P}_{vibration}) + u^2(\hat{P}_{power}) + u^2(\hat{P}_{misc}) \end{aligned} \tag{5}$$

gives the combined standard uncertainty of the pressure measurement[4]. The eight terms at the right hand side of Eq. (5) account, respectively, for uncertainties related to (a) the pressure transmitter (hysteresis, terminal-based linearity, repeatability, pressure calibration laboratory), (b) stability of the pressure transmitter, (c) radio-frequency interference (RFI) effects, (d) temperature effects, (e) atmospheric pressure, (f) vibration effects, (g) power supply effects, and (h) miscellaneous effects (mounting, etc.). With exception for (c) and (e), information on these input uncertainties may be provided by the instrument manufacturer or calibration laboratory, cf. e.g. [20].

### 3.2 Temperature element / transmitter uncertainty

The relative combined standard uncertainty of the temperature measurement is given as $E_T \equiv u_c(\hat{T})/\hat{T}$, where [1,10]

$$\begin{aligned} u_c^2(\hat{T}) = {} & u^2(\hat{T}_{elem,transm}) + u^2(\hat{T}_{stab,transm}) + u^2(\hat{T}_{RFI}) + u^2(\hat{T}_{temp}) + u^2(\hat{T}_{stab,elem}) \\ & + u^2(\hat{T}_{vibration}) + u^2(\hat{T}_{power}) + u^2(\hat{T}_{cable}) + u^2(\hat{T}_{misc}) \end{aligned} \tag{6}$$

gives the combined standard uncertainty of the temperature measurement. The nine terms at the right hand side of Eq. (6) account, respectively, for uncertainties related to (a) the temperature element and transmitter calibrated as a unit, (b) stability of the temperature transmitter, (c) RFI effects, (d) temperature effects, (e) stability of the Pt100 element, (f) vibration effects, (g) power supply effects, (h) lead resistance effects, and (i) miscellaneous effects. With exception for (c), information on these input uncertainties may be provided by the instrument manufacturer or calibration laboratory, cf. e.g. [21].

### 3.3 Densitometer uncertainty

The relative combined standard uncertainty of the density measurement is given as $E_\rho \equiv u_c(\hat{\rho})/\hat{\rho}$, where [1,10]

$$\begin{aligned} u_c^2(\hat{\rho}) = {} & s_{\rho u}^2 u^2(\hat{\rho}_u) + u^2(\hat{\rho}_{stab}) + u^2(\hat{\rho}_{rept}) + s_{\rho,T_d}^2 u_c^2(\hat{T}_d) \\ & + s_{\rho,P_d}^2 u_c^2(\hat{P}_d) + u^2(\hat{\rho}_{temp}) + +u^2(\hat{\rho}_{pres}) + u_c^2(\hat{\rho}_{inst}) + u^2(\hat{\rho}_{misc}) \end{aligned} \tag{7}$$

gives the combined standard uncertainty of the density measurement. In addition to the usual frequency relationship regression curve, the functional relationship of the vibrating-element liquid densitometer used here accounts for temperature correction and pressure correction [1,10].

---

[3] With respect to symbol notation, the *Handbook* deviates in a few cases from the recommendations given in [2], mainly for practical reasons. E.g., for relative standard uncertainties and rel. sensitivity coefficients, the symbols "$E_x$" and "$s_x^*$" are used in [1], whereas the recommended symbols in [2] are "$u(x)/x$" and "$c_x^*$", respectively.

[4] To distinguish between a quantity and an estimated value of the quantity, the symbol "$\hat{x}$" (the "hat notation") is used here to denote the estimated value of the quantity "$x$".

The nine terms at the right hand side of Eq. (7) account, respectively, for uncertainties related to (a) the indicated (uncorrected) density (calibration laboratory instruments, reading error during calibration, hysteresis, etc.) (also referred to as the "densitometer accuracy" [22]), (b) stability, (c) repeatability, (d) temperature measurement in the densitometer, $T_d$, (e) pressure measurement in the densitometer, $P_d$, (f) the temperature correction model, (g) the pressure correction model, (h) temperature and pressure effect of an on-line installation (by-pass) of the densitometer, and (i) miscellaneous effects (reading error, deposits, corrosion, vibrations, power supply variations, self-induced heat, flow in by-pass line, etc.). The various $s_{x,y}$ terms are sensitivity coefficients given in [1].

Figures for the input uncertainties $u(\hat{\rho}_u)$, $u(\hat{\rho}_{stab})$, $u(\hat{\rho}_{rept})$, $u(\hat{\rho}_{temp})$, $u(\hat{\rho}_{pres})$ and $u_c(\hat{\rho}_{inst})$ and contributions to $u(\hat{\rho}_{misc})$ should normally be provided by the instrument manufacturer or the calibration laboratory, cf. e.g. [22]. $u_c(\hat{P})$ and $u_c(\hat{T})$ are given by Eqs. (5)-(6).

### 3.4 Proving uncertainty

In Eq. (4a), the relative combined standard uncertainty related to proving of the USM is given by [1]

$$E^2_{proving} \equiv E^2_{C_{dev,j}} + E^2_{Q_{prover,j}} + \left(E^{proving}_{rept,j}\right)^2 . \tag{8}$$

The three terms at the right hand side of Eq. (8) account, respectively, for uncertainties related to (a) the deviation factor, (b) the prover measurement at proving flow rate no. *j, j = 1,…,M* (representing the uncertainty of the prover), and (c) the repeatability at proving flow rate no. *j*, *j* = 1, …, *M*. In practice $E^{proving}_{rept,j}$ represents the relative standard deviation of the spread of measured flow rates, at proving flow rate no. *j* (due to random effects related to the USM and the prover).

The deviation factor $C_{dev,j}$ represents the uncorrected deviation between the USM measurement and the "deviation curve" resulting from proving the USM at the *M* proving points, after correction of the USM measurement by the correction factor $C_{prov}$ has been made. It can be shown [1] that the relative standard uncertainty of the deviation factor may be expressed as

$$E_{C_{dev,j}} = \frac{1}{\sqrt{3}}\left|\frac{Dev_{C,j}}{\hat{C}_{dev,j}}\right| \approx \frac{Dev_{C,j}}{\sqrt{3}} , \qquad Dev_{C,j} = \frac{C_{prov}\cdot Q^{proving}_{USM,j} - Q_{prover,j}}{Q_{prover,j}} , \qquad j = 1, \ldots, M, \tag{9}$$

where $Q^{proving}_{USM,j}$ is the standard volumetric flow rate measured by the USM under proving, at proving flow rate no. *j*, $Q_{prover,j}$ is the standard volumetric flow rate as measured by the prover, $Dev_{C,j}$ is the corrected relative deviation at this test flow rate (i.e. the relative deviation after multiplication with the proving correction factor, $C_{prov}$), and $C_{dev,j} = 1 + Dev_{C,j}$ is the deviation factor. The deviation data $Dev_{C,j}$, *j = 1, …, M*, are available from proving at the *M* proving flow rates. Details are given in [1].

The relative combined standard uncertainty of the prover volumetric flow rate measurement at proving flow rate no. *j* is given by [1]

$$E^2_{Q_{prover,j}} \equiv E^2_{BV} + E^2_{\Delta t_p} + E^2_{C_{tsp}} + E^2_{C_{psp}} + E^2_{C_{tlp}} + E^2_{C_{plp}} + correlation\ terms\ C \ . \tag{10}$$

In Eq. (10), "correlation terms C" refer to correlations between the volume correction factors, such as (a) temperature correlations between $C_{tsp}$ and $C_{tlp}$, $C_{tsp}$ and $C_{plp}$, $C_{tlp}$ and $C_{plp}$, (b) pressure correlations between $C_{psp}$ and $C_{plp}$, and (c) density correlation between $C_{tlp}$ and

$C_{plp}$ [1]. Such correlations are neglected in the simplified calculation example given here, cf. Section 5.

### 3.5 USM duty operation uncertainty

In Eq. (4a), the relative combined standard uncertainty of the USM in duty operation is given by [1]

$$E_{USM}^2 \equiv E_{rept}^2 + E_{USM,\Delta}^2 + E_{misc}^2 \,. \tag{11}$$

The three terms at the right hand side of Eq. (11) account, respectively, for uncertainties related to (a) repeatability of the USM measurement in duty operation, at the flow rate in question (due to random transit time effects), (b) systematic effects in duty operation of the USM, due to change of conditions from proving to duty operation, and (c) miscellaneous systematic effects on the USM duty measurement which are not eliminated by proving, and which are not covered by other uncertainty terms accounted for here (e.g. inaccuracy of the USM functional relationship (the underlying mathematical model), etc.).

In Eq. (11), the "USM duty repeatability" term is given by

$$E_{rept}^2 \equiv 2\sum_{i=1}^{N} (s_{t1i}^* E_{t1i,U})^2 \,. \tag{12}$$

The relative sensitivity coefficient $s_{t1i}^*$ is given in [1]. $E_{t1i,U}$ is the relative standard uncertainty of those contributions to the transit times of path no. *i* which are uncorrelated with respect to upstream and downstream propagation. It is given as

$$E_{t1i,U} = u(\hat{t}_{1i}^{random}) / \hat{t}_{1i} \,, \tag{13}$$

where $\hat{t}_{1i}$ is the upstream transit time of path no. *i*, and and $u(\hat{t}_{1i}^{random})$ is the standard uncertainty due to in-duty random effects on transit times (after possible signal averaging), such as (a) turbulence, (b) incoherent noise (due to pressure reduction valves, RFI, vibrations, etc.), (c) coherent noise (acoustical and electrical cross-talk, acoustic reverberation, other signal interference), (d) finite clock resolution, (e) electronics stability (possible random effects), (f) possible random effects in signal detection/processing (e.g. erroneous signal period identification), and (g) power supply variations. In practice, at a given flow rate, $u(\hat{t}_{1i}^{random})$ represents the standard deviation of the spread of measured transit times in path no. *i*. Similarly, $E_{rept}$ represents the standard deviation of the spread of measured flow rates, at the actual flow rate.

In Eq. (11), the "systematic USM duty effects" term can be expressed by[5]

$$E_{USM,\Delta}^2 \equiv E_{body,\Delta}^2 + E_{time,\Delta}^2 + E_{I,\Delta}^2 \,, \tag{14}$$

where the three terms at the right hand side of Eq. (14) account, respectively, for uncertainties related to (a) possible uncorrected change of the USM meter body dimensions (radius, lateral chord positions, inclination angles) from proving to duty operation, caused by possible deviation in *P*, *T* between proving and duty operation, (b) possible uncorrected systematic effects on the transit times caused e.g. by deviation in conditions from proving to duty operation (*P*, *T*, transducer deposits, transducer ageing, etc), and (c) possible change of installation conditions from proving to duty operation (related to the USM integration method).

[5] The subscript "$\Delta$" denotes that *only deviations relative to the conditions at proving* are to be accounted for in the expressions involving this subscript. That means, uncertainty contributions which are practically eliminated by proving, are *not* to be included in these expressions.

In Eq. (14), the "meter body uncertainty" term can be shown [1] to be given as

$$E_{body,\Delta} \equiv E_{rad,\Delta} + E_{chord,\Delta} + E_{angle,\Delta} \ , \tag{15a}$$

where

$$E_{rad,\Delta} \equiv s_R^* E_{R,\Delta} \ , \qquad E_{chord,\Delta} \equiv \sum_{i=1}^{N} sign(\hat{y}_i) s_{yi}^* E_{yi,\Delta} \ , \qquad E_{angle,\Delta} \equiv \sum_{i=1}^{N} sign(\hat{\phi}_i) s_{\phi i}^* E_{\phi i,\Delta} \ , \tag{15b}$$

$$E_{R,\Delta}^2 = E_{yi,\Delta}^2 = E_{KP}^2 + E_{KT}^2 \ , \qquad E_{\phi i,\Delta} = \frac{B \sin 2\hat{\phi}_{i0}}{2\hat{\phi}_{i0}} E_{KP} \ . \tag{15c}$$

Here, $s_R^*$, $s_{yi}^*$ and $s_{\phi i}^*$ are relative sensitivity coefficients given in [1], $\phi_{i0}$ is the inclination angle of path no. *i* at "dry calibration" conditions, *N* is the number of acoustic paths in the USM, and *B* is a constant defined in [1]. $E_{KP}$ and $E_{KT}$ are the relative standard uncertainties of the radial pressure and temperature correction factors for the USM meter body, $K_P$ and $K_T$, respectively, given as

$$E_{KP} \equiv u_c(\hat{K}_P)/\hat{K}_P \ , \qquad u_c(\hat{K}_P) = \sqrt{(\Delta\hat{P}_{cal})^2 u^2(\hat{\beta}) + \hat{\beta}^2 u_c^2(\Delta\hat{P}_{cal})} \ , \tag{16a}$$

$$E_{KT} \equiv u_c(\hat{K}_T)/\hat{K}_T \ , \qquad u_c(\hat{K}_T) = \sqrt{(\Delta\hat{T}_{cal})^2 u^2(\hat{\alpha}) + \hat{\alpha}^2 u_c^2(\Delta\hat{T}_{cal})} \ , \tag{16b}$$

where $u(\hat{\alpha})$ and $u(\hat{\beta})$ are the standard uncertainties of the coefficients of linear temperature and pressure expansion of the meter body material (usually steel), $\alpha$ and $\beta$, respectively. $\Delta P_{cal}$ and $\Delta T_{cal}$ are the difference in pressure and temperature between line and proving conditions, respectively. For calculation of the combined standard uncertainties of $\Delta P_{cal}$ and $\Delta T_{cal}$, two cases are addressed here. In cases for which *P* and *T* corrections of the meter body are *not* used, these uncertainties are determined by the *span* of $\Delta P_{cal}$ and $\Delta T_{cal}$, so that

$$u_c(\Delta\hat{P}_{cal}) = \Delta\hat{P}_{cal}/\sqrt{3} \ , \qquad u_c(\Delta\hat{T}_{cal}) = \Delta\hat{T}_{cal}/\sqrt{3} \ . \tag{17}$$

In cases where *P* and *T* corrections of the meter body *are* used, these uncertainties are determined by the *measurement uncertainties* of $\Delta P_{cal}$ and $\Delta T_{cal}$, so that

$$u_c(\Delta\hat{P}_{cal}) = \sqrt{2} u_c(\hat{P}) \ , \qquad u_c(\Delta\hat{T}_{cal}) = \sqrt{2} u_c(\hat{T}) \ , \tag{18}$$

where $u_c(\hat{P})$ and $u_c(\hat{T})$ are given by Eqs. (5)-(6). Details are given in [1].

In Eq. (14), the "systematic transit time effects" term is given as

$$E_{time,\Delta} \equiv \sum_{i=1}^{N} \left( s_{t1i}^* E_{t1i,C}^{\Delta} + s_{t2i}^* E_{t2i,C}^{\Delta} \right) \ . \tag{19}$$

$E_{t1i,C}^{\Delta}$ and $E_{t2i,C}^{\Delta}$ are the relative standard uncertainties of uncorrected systematic transit time effects on upstream and downstream propagation of acoustic path no. *i*, due to possible deviation in pressure and/or temperature from proving to duty operation, defined as

$$E_{t1i,C}^{\Delta} = u(\hat{t}_{1i}^{systematic})/\hat{t}_{1i} \ , \qquad E_{t2i,C}^{\Delta} = u(\hat{t}_{2i}^{systematic})/\hat{t}_{2i} \ . \tag{20}$$

$\hat{t}_{1i}$ and $\hat{t}_{2i}$ are the upstream and downstream transit times of path no. *i*, and $u(\hat{t}_{1i}^{systematic})$ and $u(\hat{t}_{2i}^{systematic})$ are the standard uncertainties of uncorrected systematic effects in these transit times. Information on these input uncertainties should be provided by the USM manufacturer. $s_{t1i}^*$ and $s_{t2i}^*$ are relative sensitivity coefficients defined in [1].

Such systematic transit time effects may be due to (a) cable/electronics/transducer/diffraction time delay (due to line pressure and temperature effects, ambient temperature effects, drift, effects of possible transducer exchange), (b) possible $\Delta t$-correction (line pressure and temperature effects, ambient temperature effects, drift, reciprocity effects, effects of possible transducer exchange), (c) possible systematic effects in signal detection/processing, (d) possible cavity time delay correction effects, (e) possible transducer deposits (wax, scaling, etc.), and (f) sound refraction (flow profile effects ("ray bending")).

In Eq. (14), the "installation effects" term $E_{I,\Delta}$ is related to the USM integration method, and serves as an input uncertainty. Such installation effects on the USM integration uncertainty may be due to (a) change of *axial flow velocity profile* (from proving to duty operation), and (b) change of *transversal flow velocity profiles* (from proving to duty operation). Such changes may be due to e.g. (*i*) line pressure and temperature effects, (*ii*) ambient temperature effects, (*iii*) possible changed wall roughness over time (corrosion, wear, pitting, etc.), in the pipe and meter body, and (i*v*) possible wall deposits / contamination in the pipe and meter body (wax, scaling), etc.

### 3.6 Signal communication and flow computer uncertainties

In Eqs. (4a), the relative uncertainty term $E_{comm}$ accounts for the uncertainties due to the signal communication between the USM field electronics and the flow computer (e.g. the flow computer calculation of frequency in case of analog frequency output). $E_{flocom}$ accounts for the uncertainty of the flow computer calculations. Both should be specified by the USM manufacturer, and are normally relatively small.

## 4 MICROSOFT EXCEL PROGRAM "*EMU - USM FISCAL OIL METERING STATION*"

A PC program has been implemented based on the uncertainty model for the metering station described in Section 3. The program *EMU - USM Fiscal Oil Metering Stations* is implemented as a Microsoft Excel 2003 spreadsheet.

The program calculates the expanded and relative expanded uncertainties of an oil metering station which is based on a proved USM, for the three measurands in question, $q_v$, $Q_v$ and $q_m$.

In addition to calculation/plotting/reporting of the expanded uncertainty of the oil metering station and the individual instruments of the station, the Excel program can be used to calculate, plot and analyse the relative importance of the various contributions to the uncertainty budget for the various instruments of the metering station (using bar-charts).

For several of the instruments and procedures involved in the metering station, an implementation strategy has been chosen which enables the user to give uncertainty input at two levels: (1) an *"overall level"*, and (2) a more *"detailed level"*, cf. Table 3. This provides a useful flexibility in use of the program.

At the *overall level*, the user specifies the combined standard uncertainty of the instrument in question directly as input to the program. It is left to the user to calculate and document this uncertainty figure. This option is general, and covers any method of obtaining the uncertainty figure[6].

[6] The "overall level" option may be of interest in several cases, such as e.g.: (a) if the user wants a "simple" and quick evaluation of the influence of an instrument uncertainty on the expanded (overall) uncertainty of the oil metering station, (b) in case of a different installation of the oil densitometer (e.g. in-line), (c) in case of a different oil densitometer functional relationship, or (d) in case the input used at the "detailed level" does not fit sufficiently well to the type of input data / uncertainties which are relevant for e.g. the pressure transmitter or temperature element/transmitter at hand.

At the *detailed level*, the combined standard uncertainty of the instrument in question is calculated by the program, from more basic input for the instrument provided e.g. by the instrument manufacturer and calibration laboratory, as outlined in Section 3.

Table 3. Uncertainty model contributions, and optional levels for specification of input uncertainties to the program *EMU - USM Fiscal Oil Metering Stations*.

| Uncertainty contribution | Overall level | Detailed level |
|---|---|---|
| Pressure measurement uncertainty (in each of: meter run, densitometer and prover) | ✓ | ✓ |
| Temperature measurement uncertainty (in each of: meter run, densitometer and prover) | ✓ | ✓ |
| Density measurement uncertainty | ✓ | ✓ |
| Reference density calculation | ✓ | ✓ |
| Prover uncertainty | ✓ | ✓ |
| Proving uncertainty | | ✓ |
| USM duty operation uncertainty | ✓ | ✓ |
| Signal communication and flow computer calculations | ✓ | |

With respect to *USM proving* and *USM duty operation*, the level for specification of input uncertainties at the detailed level is adapted to data available from duty operation, proving and from the USM manufacturer. In particular this concerns:

(1) USM proving:

- **Prover.** The user specifies a number of input uncertainties needed for calculation of the prover uncertainty, $E_{Q_{prover}}$, cf. Eq. (10).
- **Repeatability.** The user specifies the repeatability (relative standard deviation) of the indicated USM flow rate measurement at proving, $E_{rept,j}^{proving}$, cf. Eq. (8). That is, the combined repeatability of the USM and the prover. It can be given in the program to be flow rate dependent.
- **Deviation factor.** The user specifies the corrected relative deviation $Dev_{C,j}$ at each proving flow rate ("proving point"), i.e. the relative deviation from reference after multiplication with the "proving correction factor", $C_{prov}$, cf. Eq. (9).

(2) USM duty operation:

- **Repeatability.** The user specifies either (a) the repeatability (relative standard deviation) of the indicated USM flow rate measurement in duty operation, $E_{rept}$, or (b) the repeatability (standard deviation) of the measured transit times, $u(\hat{t}_{1i}^{random})$, cf. Eqs. (12) and (13), respectively. Both can be given in the program to be flow rate dependent.
- **Meter body parameters.** The user specifies whether correction for pressure and temperature effects is used or not for the USM meter body, and the uncertainties of the temperature and pressure expansion coefficients, $u(\hat{\alpha})$ and $u(\hat{\beta})$. Cf. Eqs. (15)-(18).
- **Systematic transit time effects.** The user specifies the uncertainty of uncorrected systematic effects on the measured upstream and downstream transit times, $u(\hat{t}_{1i}^{systematic})$ and $u(\hat{t}_{2i}^{systematic})$, cf. Eqs. (20). Only changes from proving to duty operation are relevant.
- **Integration method (installation effects).** The user specifies the uncertainty related to the integration method / installation effects, $E_{I,\Delta}$, cf. Eq. (14). Only changes from proving to duty operation are relevant here.

With respect to the USM technology, the program can thus be run in two modes:

(A) Completely meter independent, and
(B) Weakly meter dependent.

Mode (A) corresponds to choosing the overall level for the USM duty operation uncertainty (both for the repeatability and the systematic deviation re. proving). Mode (B) corresponds to choosing the "detailed level".

By “weakly meter dependent” is here meant that the inner diameter, number of paths and the number of reflections for each path are to be known. However, actual values for the inclination angles, lateral chord positions and integration weights do not need to be known. Only very approximate values for these quantities are needed (used for calculation of certain sensitivity coefficients).

## 5 UNCERTAINTY EVALUATION EXAMPLE

As an example of evaluation of the expanded uncertainty of a USM fiscal oil metering station using the EMU program described in Section 4, consider the metering station instrumentation example given in Table 2: 8” pipeline, a 8" USM duty meter with flow computer, a 20" prover, a Rosemount 3051P Reference Class Pressure Transmitter [20], a Pt 100 4-wire RTD element and a Rosemount 3144 Smart Temperature Transmitter [21], and an on-line (by-pass) installed Solartron 7835 Liquid Density Transducer [22]. The type of flow computer and prover are arbitrary (unspecified). The diameter and actual volume of the 20" prover is 0.5 m and 7 $m^3$, respectively. The 8" USM is a 0.20 m diam. 4-path meter with parallel chords, non-reflecting paths and Gauss-Jacobi integration. A typical North Sea oil is considered [10], with density 776 $kg/m^3$ at densitometer conditions. Line conditions (in the meter run) are taken to be 18 barg and 65 $^oC$. Densitometer conditions are 17.5 barg and 63 $^oC$. Proving conditions are taken to be 18 bara and 65 $^oC$ (for the USM and the prover).

Evaluation of e.g. the relative expanded uncertainty of the axial volumetric flow rate, $kE_{q_v}$, according to Eq. (4a), involves the USM, the prover, the pressure and temperature measurements, the densitometer, the signal communication / flow computer, and the oil parameters. The “detailed level” of input is used here. 6 proving flow velocities are considered, in the range 0.4 – 10 m/s (corresponds to actual volumetric flow rates of about 45 – 1131 $m^3/h$).

For the proving of the USM, a number of input uncertainties are in question, cf. Eqs. (8) and (10). The deviation factor uncertainty, $kE_{C_{dev,j}}$, is taken to be 0.02 % (100 % conf. lev., rect. distrib.)[7]. The repeatability (standard uncertainty, i.e. standard deviation) of the proving measurement, $E_{rept,j}^{proving}$, is taken to be 0.02 % at all proving flow rates (which is probably simplified). The relative standard uncertainty of the prover volume, $E_{BV}$, is taken to be 0.019 %. The standard uncertainty of the proving time period, $\Delta t_p$, is taken to be 1 ms. The standard uncertainties of the thermal expansion coefficient and the modulus of elasticity of the prover steel body are both taken to be 11.5 %. The standard uncertainties of the inner diameter and wall thickness of the prover are both taken to be 0.5 %.

With respect to the oil parameters, a relatively large number of input uncertainties are to be specified. The relative standard uncertainties of all oil temperature and pressure measurements (in the meter, densitometer and the prover), $E_T$ and $E_P$, are taken to be 0.023 % and 0.044 %, respectively. Due to space limitations, it is referred to [1] for details on other oil parameter input uncertainties.

For the USM in duty operation, the input uncertainties in question are given by Eqs. (11)-(20). The USM repeatability in duty operation is tentatively taken to be $E_{rept}$ = 0.02 % (standard deviation), constant over the flow rate range (which is probably simplified). The relative standard uncertainty of the integration method (accounting for possible changes in installation effects from proving to duty operation) is taken to be $E_{I,\Delta}$ = 0.01 %, as a tentative and possibly large example value. The uncertainties of uncorrected systematic effects on the measured upstream and downstream transit times (accounting for possible changes from

[7] In the present calculation example given here, all input uncertainties given in the text are taken to correspond to 67 %, 95 % or 100 % confidence levels (depending on type of uncertainty), with normal or rectangular probability distribution, and coverage factor *k* = 1, 2 or $\sqrt{3}$, respectively.

proving to duty operation), $k \cdot u(\hat{t}_{1i}^{systematic})$ and $k \cdot u(\hat{t}_{2i}^{systematic})$, are given as 10 and 9.5 ns (100 % conf. lev., rect. distrib.), respectively, as a tentative example. The case is considered where pressure and temperature correction is used for the meter body. The uncertainties of the temperature and pressure expansion coefficients $k \cdot u(\hat{\alpha})$ and $k \cdot u(\hat{\beta})$ are set to 20 % (100 % conf. lev., rect. distrib.), as example values. Details are given in [1].

The standard uncertainties related to the flow computer and signal communication are set to zero in this example.

Fig. 1 shows the relative expanded uncertainty of the volumetric flow rate measurement for this illustration example (together with the volumetric flow rate itself), plotted over the flow velocity range 0.4 to 10 m/s. The relative expanded uncertainty is calculated at *M* = 6 flow velocities for which proving has been performed, and straight lines are drawn in-between these points.

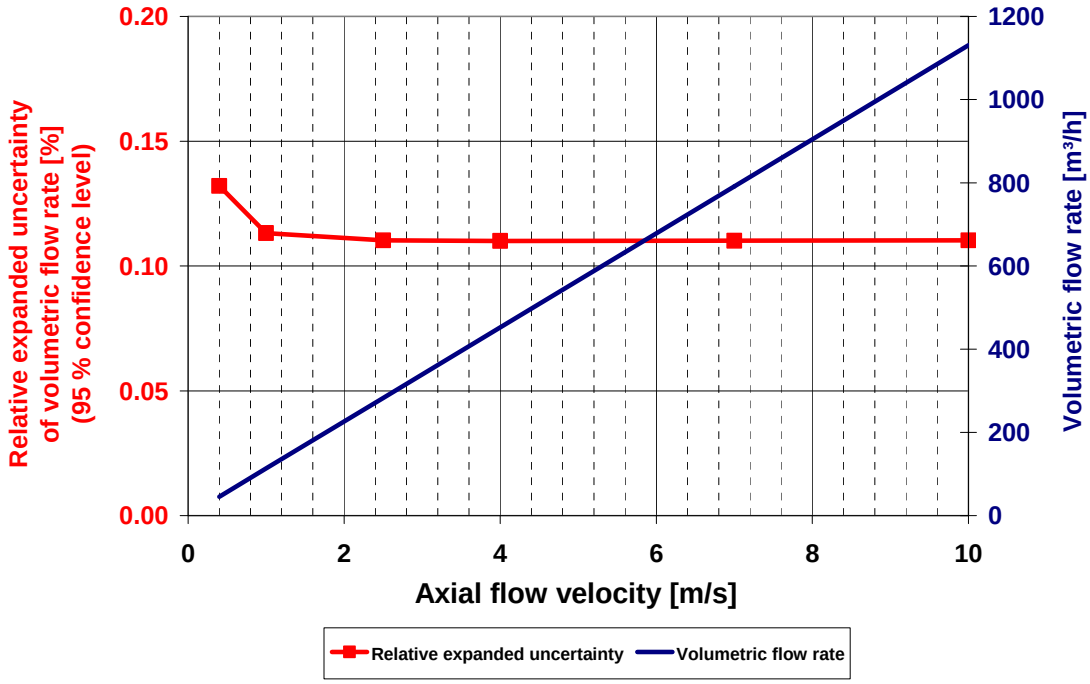


Fig. 1. Illustration example of volumetric flow rate measurement, $q_v$, and its corresponding relative expanded uncertainty, $kE_{q_v}$. The markers indicate the 6 flow rates at which proving has been made ("proving points").

The various contributions to the relative expanded uncertainty of the volumetric flow rate measurement may be investigated in further detail at each of the *M* = 6 "proving points" shown by markers in Fig. 1. The bar-chart shown in Fig. 2 gives the relative importance of such contributions at a flow velocity of 1 m/s. At this flow velocity, two uncertainty contributions dominate the uncertainty budget in this illustration and tentative example: the prover uncertainty and the systematic deviation of the USM in duty operation relative to proving, followed by the repeatability contributions at proving and in duty operation.

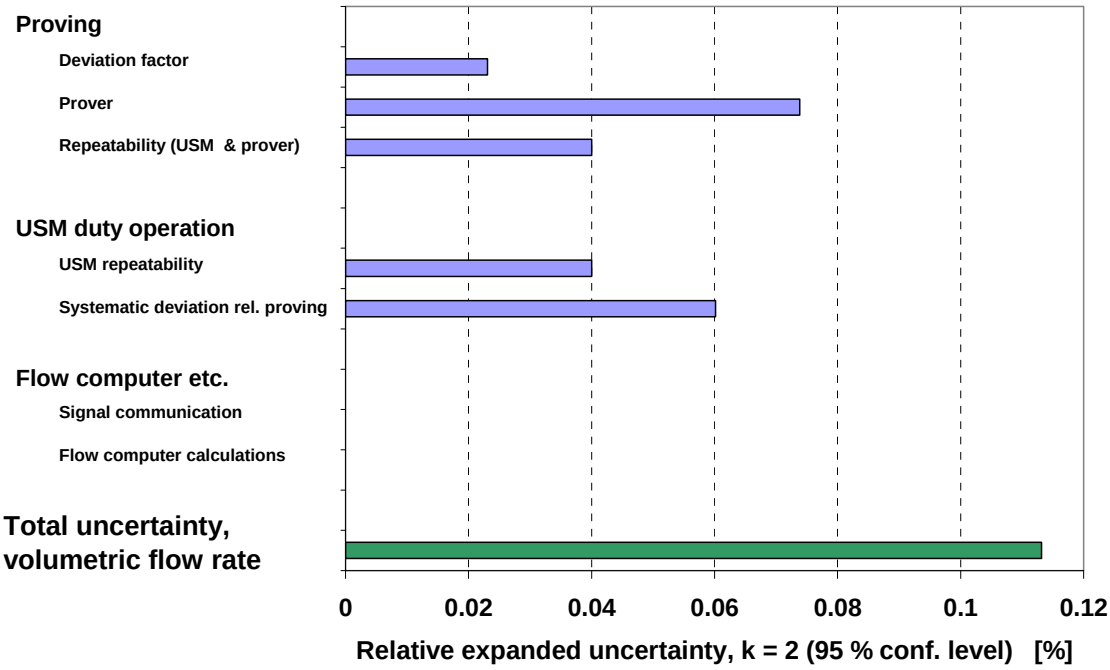


Fig. 2. Bar-chart showing contributions to the calculated relative expanded uncertainty of the volumetric flow rate measurement, at 1 m/s flow velocity.

In Fig. 2 the relative expanded uncertainty of prover measurement is calculated to about 0.074 %. It may be of interest to investigate the relative importance of the various contributions to this uncertainty figure. Fig. 3 shows the contributions to the expanded uncertainty of the prover, calculated according to Eq. (10). It appears that in this illustration example the prover uncertainty is dominated by the uncertainty of $C_{tlp}$, followed by the uncertainties of $C_{tsp}$ and the prover "base volume", *BV*. Other uncertainty contributions are relatively smaller.

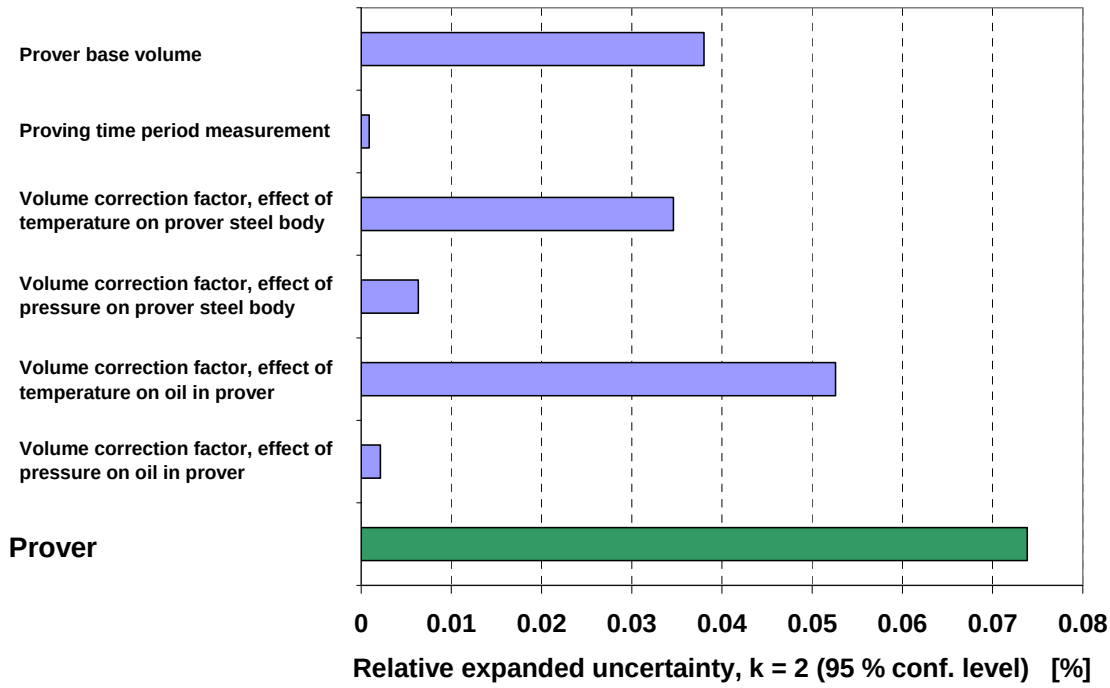


Fig. 3. Bar-chart showing the various contributions to the expanded uncertainty of the prover measurement, at 1 m/s flow velocity, calculated according to Eq. (10).

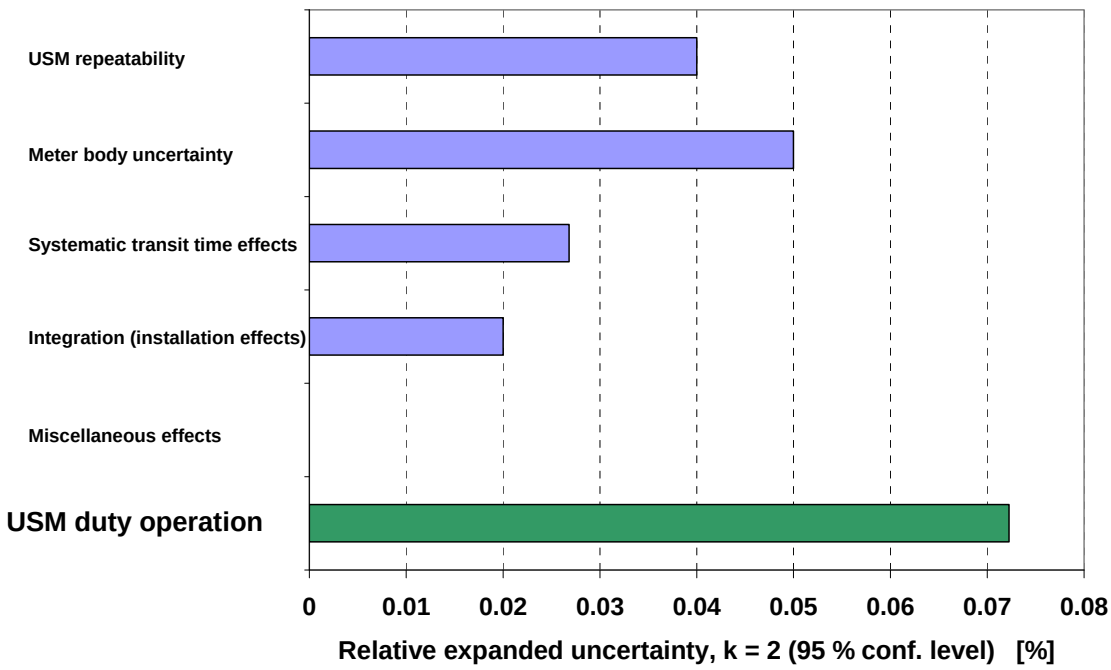


Fig. 4. Bar-chart showing the various contributions to the expanded uncertainty of the USM field measurement, at 1 m/s flow velocity, calculated according to Eqs. (11)-(20).

To investigate the relative expanded uncertainty of the USM duty measurement shown in Fig. 2 in some more detail, Fig. 4 shows the contributions to this uncertainty, calculated according to Eqs. (11)-(20). In addition to the miscellaneous effects, these are organized in four groups: USM repeatability in duty operation, meter body uncertainty, uncertainty of systematic transit time effects, and the integration method uncertainty (installation effects). In the present example four groups all contribute to the USM duty uncertainty. In general the latter two groups are the most difficult to specify (only the USM repeatability is normally available from current USM manufacturer data sheets), and only tentative uncertainty figures have been used in the present calculation example, to illustrate use of the program, and demonstrate the sensitivity to these uncertainty contributions.

Table 4 summarizes the calculation results of this example in an overall uncertainty budget. It appears that the proving and USM duty uncertainties contribute almost equally to the relative expanded uncertainty of the volumetric flow rate measurement, at this flow velocity.

Table 4. Illustration example of an overall uncertainty budget for the USM fiscal oil metering station, for the volumetric flow rate, $q_v$, for a flow velocity of 1 m/s.

| Source | Uncertainty contribution | | | | Combined uncertainty | |
|---|---|---|---|---|---|---|
| | Relative expanded uncertainty | Confidence level & probab. distribution | Cover. factor, *k* | Relative standard uncertainty | Rel. sens. coeff. | Relative Variance |
| Proving | 0.0871 % | 95 % (normal) | 2 | 0.0436 % | 1 | $1.897 \cdot 10^{-7}$ |
| USM duty operation | 0.0722 % | 95 % (normal) | 2 | 0.0361 % | 1 | $1.305 \cdot 10^{-7}$ |
| Signal comm. / flow comp. | Neglected | - | - | - | 1 | 0 |
| Sum of relative variances | | | | $E_{q_v}^2$ | | $3.206 \cdot 10^{-7}$ |
| Relative combined standard uncertainty | | | | $E_{q_v}$ | | 0.057 % |
| Relative expanded uncertainty (95 % confidence level, *k* = 2) | | | | $k \cdot E_{q_v}$ | | **0.113 %** |

The uncertainty evaluation example discussed above for illustration purposes, address the volumetric flow rate, $q_v$. Similar analyses can be made for the standard volumetric flow rate, $Q_v$, and the mass flow rate, $q_m$.

Calculations of this type may be made for the pressure transmitter and the temperature element/transmitters (in the meter run, the densitometer and the prover), the densitometer, the reference density, the prover, and the proving of the USM. For documentation purposes, necessary reporting of input data and calculated results are available, for the three measurands given by Eqs. (1).

## 6 CONCLUSIONS

The NPD regulations states that "it shall be possible to document the total uncertainty of the measurement system. An uncertainty analysis shall be prepared for the measurement system within a 95 % confidence level" [4]. The *GUM* [2] put requirements to such documentation. To meet such requirements and harmonize procedures and industry practice in the documentation of fiscal measurements, a series of handbooks on uncertainty calculation of fiscal oil and gas metering stations is developed in a cooperation between NFOGM, NPD, Tekna and CMR [8-10,1].

In the present paper, the ongoing development of a handbook of uncertainty calculations of ultrasonic fiscal oil metering stations [1] is described. Three different metering station scenarios are being addressed in [1]:

Scenario A: A USM "duty meter" which is *in-situ* calibrated using a prover, typically every 4th day.

Scenario B: A USM "duty meter" which is operated together with a USM "master meter". The USM "duty meter" is *in-situ* calibrated vs. the USM "master meter". The USM "master meter" is *in-situ* calibrated vs. a prover, typically once a year.

Scenario C: A USM "duty meter" which is operated together with a turbine (TM) "master meter". The USM "duty meter" is *in-situ* calibrated vs. the TM "master meter". The TM "master meter" is *in-situ* calibrated vs. a prover, typically once a year.

The present paper gives a description of Scenario A, including an uncertainty calculation example. The example is meant essentially to illustrate and demonstrate the possibilities of the *Handbook* and the accompanying *EMU* program, and does not serve as an uncertainty analysis of a USM fiscal oil metering station.

The expanded uncertainties calculated by the program *EMU - USM Fiscal Oil Metering Stations* may be used in documentation of the metering station uncertainty. That means, provided the user of the program (on basis of manufacturer information or other sources) can document the numbers used for the input uncertainties to the program, the *Handbook* and the program gives procedures for propagation of these input uncertainties.

For traceability purposes the input data to the program (quantities and uncertainties) must be documented by the user. The user must also document that the calculation procedures and functional relationships implemented in the program are in conformity with the ones actually applied in the fiscal oil metering station[8].

The uncertainty model for USM fiscal oil metering stations presented in the *Handbook* is based on present-day "state of the art of knowledge" for stations of this type, and is not expected to be complete with respect to description of effects influencing on such metering stations. In spite of that, the uncertainty model does account for a large number of the important factors that influence on the expanded uncertainty of metering stations of this type. It is expected that the most important uncertainty contributions have been accounted for. Evaluation of the effects of these factors on the uncertainty of the metering station should be possible with the uncertainty model and the program developed here.

[8] If the "overall level" options of the program are used, the program should cover a wide range of situations met in practice.

It is the intention and hope of the partners presenting this *Handbook* that - after a period of practical use of the *Handbook* and the program - the uncertainty model presented here will be subject to necessary comments and viewpoints from users and developers of USMs, and others with interest in this field, as a basis for a possible later revision of the *Handbook*. The overall objective of such a process would of course be that - in the end - a useful and accepted method for calculation of the uncertainty of USM fiscal oil metering stations can be agreed on, in the Norwegian metering society as well as internationally.

## SYMBOL NOTATION

$q_v$ : axial volumetric flow rate at line conditions [$m^3$/h],

$Q_v$ : axial volumetric flow rate at standard reference conditions (1 atm. and 15 $^oC$) [$Sm^3$/h],

$q_m$ : axial mass flow rate [kg/h],

$q_{USM}$ : axial volumetric flow rate indicated by the USM under duty operation (line conditions), before the "proving correction factor" $C_{prov}$ is applied [$m^3$/s],

$\rho$ : oil density in the meter run (line conditions) [kg/$m^3$],

$\rho_d$ : oil density in the densitometer [kg/$m^3$],

$\rho_{ref}$ : oil density at standard reference conditions (1 atm. and 15 $^oC$) [kg/$m^3$],

$C_{prov}$ : correction factor accounting for proving of the USM (Scenario A) (here referred to as the "proving correction factor") [-],

$C_j^{prov}$ : meter factor determined in proving of the USM (Scenario A), $j$ = 1, …, $M$ [-],

$K_{prov,j}^{USM}$ : K-factor of the ultrasonic meter (USM) at proving test flow rate no. $j$, $j = 1$, …, $M$, determined in proving of the USM [pulses/$m^3$],

$K_{DFC}$ : DFC (digital-to-frequency converter) factor [pulses/$m^3$],

$M$ : number of proving flow rates ("proving points"),

$C_{tlm}$ : Volume correction factor (VCF) for the effect of temperature on the liquid (oil) in the meter, re. standard reference conditions [-],

$C_{plm}$ : Volume correction factor (VCF) for the effect of pressure on the liquid (oil) in the meter, re. standard reference conditions [-],

$C_{tld}$ : Volume correction factor (VCF) for the effect of temperature on the liquid (oil) in the densitometer, re. standard reference conditions [-],

$C_{pld}$ : Volume correction factor (VCF) for the effect of temperature on the liquid (oil) in the densitometer, re. standard reference conditions [-].

$C_{tlp}$ : volume correction factor (VCF) for the effect of temperature on the liquid (oil) in the prover at proving conditions, re. std. reference conditions [-],

$C_{plp}$ : volume correction factor (VCF) for the effect of pressure on the liquid (oil) in the prover at proving conditions, re. standard reference conditions [-],

$C_{tsp}$ : volume correction factor (VCF) for the effect of temperature on the prover steel at proving conditions, re. std. reference conditions [-],

$C_{psp}$ : volume correction factor (VCF) for the effect of pressure on the prover steel at proving conditions, re. std. reference conditions [-],

$BV$ : Prover volume at "base conditions", taken to be standard reference conditions (1 atm., 15 $^oC$) [$m^3$],

$\Delta t_p$ : proving time period, i.e. time period between signals from the two detector switches 1 and 2 in the prover [s],

$k$ : coverage factor [-],

$E_P$ : relative combined standard uncertainty of the liquid pressure measurement [-],

$E_T$ : relative combined standard uncertainty of the liquid temperature measurement [-],

$E_\rho$ : relative combined standard uncertainty of the liquid density measurement [-],

$E_{q_v}$ relative combined standard uncertainty of the axial volumetric flow rate estimate, $\hat{q}_v$ [-],

$E_{Q_v}$ relative combined standard uncertainty of the standard axial volumetric flow rate estimate, $\hat{Q}_v$ [-],

$E_{q_m}$ relative combined standard uncertainty of the axial mass flow rate estimate, $\hat{q}_m$ [-],

$E_{proving}$ : relative combined standard uncertainty of the estimate $\hat{q}_v$ , related to proving of the USM [-],

$E_{USM}$ : relative combined standard uncertainty of the estimate $\hat{q}_v$ , related to duty operation of the USM [-],

$E_{comm}$ : relative standard uncertainty of of the estimate $\hat{q}_v$ , due to signal communication [-],

$E_{flocom}$ : relative standard uncertainty of of the estimate $\hat{q}_v$ , due to the flow computer [-],

$E_{C_{dev,j}}$ : relative combined standard uncertainty of the deviation factor estimate, $\hat{C}_{dev,j}$ , at proving flow rate no. *j*, *j* = 1, …, *M* [-],

$E_{Q_{prover,j}}$ : relative combined standard uncertainty of the prover volumetric flow rate measurement, $\hat{Q}_{prover,j}$ , at proving flow rate no. *j*, *j* = 1, …, *M* [-],

$E_{rept,j}^{proving}$ : repeatability (relative standard uncertainty, i.e. standard deviation) of the proving measurement (volumetric flow rate), at proving flow rate no. *j*, *j* = 1, …, *M* [-],

$E_{BV}$ : relative standard uncertainty of the prover "base volume" *BV* [-],

$E_{\Delta t_{p,j}}$ : relative standard uncertainty of the prover time period measurement, $\Delta t_p$ , at proving flow rate no. *j*, *j = 1, …, M* [-],

$E_{C_{tlm}}$ : relative combined standard uncertainty of the volume correction factor estimate $\hat{C}_{tlm}$ [-],

$E_{C_{plm}}$ : relative combined standard uncertainty of the volume correction factor estimate $\hat{C}_{plm}$ [-],

$E_{C_{tlp}}$ ≡ relative combined standard uncertainty of the volume correction factor estimate $\hat{C}_{tlp}$ [-],

$E_{C_{plp}}$ ≡ relative combined standard uncertainty of the volume correction factor estimate $\hat{C}_{plp}$ [-],

$E_{C_{tsp}}$ : relative combined standard uncertainty of the volume correction factor estimate $\hat{C}_{tsp}$ [-],

$E_{C_{psp}}$ ≡ relative combined standard uncertainty of the volume correction factor estimate $\hat{C}_{psp}$ [-],

$E_{rept}$ : repeatability (relative combined standard uncertainty, i.e. standard deviation) of the USM measurement in duty operation (volumetric flow rate), at the flow rate in question [-],

$E_{USM,\Delta}$ : relative standard uncertainty of the estimate $\hat{q}_v$ , related to duty operation of the USM [-],

$E_{misc}$ : miscellaneous systematic effects on the USM duty measurement which are not eliminated by proving, and which are not covered by other uncertainty terms accounted for here (e.g. inaccuracy of the USM functional relationship (the underlying mathematical model), etc.) [-],

$E_{body,\Delta}$ : relative combined standard uncertainty of the estimate $\hat{q}_v$ , due to change of the USM meter body from proving to duty operation. That is, uncertainty of the meter body inner radius, $\hat{R}$ , the lateral chord positions of the *N* acoustic paths, $\hat{y}_i$ , and the inclination angles of the *N* acoustic paths, $\hat{\phi}_i$ , *i* = 1, …, *N*, caused by possible deviation in pressure and/or temperature between proving and duty operation [-],

$E_{time,\Delta}$ : relative combined standard uncertainty of the estimate $\hat{q}_v$ , due to systematic effects on the transit times of the *N* acoustic paths, $\hat{t}_{1i}$ and $\hat{t}_{2i}$ , *i* = 1, …, *N*, caused by possible deviation in pressure and/or temperature between proving and duty operation [-],

$E_{I,\Delta}$ : relative standard uncertainty of the USM integration method due to change of installation conditions from proving to duty operation [-],

$E_{rad,\Delta}$ : relative combined standard uncertainty of the estimate $\hat{q}_v$ , due to uncertainty of the meter body inner radius, $\hat{R}$ , caused by possible deviation in pressure and/or temperature between proving and duty operation [-],

$E_{chord,\Delta}$ : relative combined standard uncertainty of the estimate $\hat{q}_v$ , due to uncertainty of the lateral chord positions of the *N* acoustic paths, $\hat{y}_i$ , *i* = 1, …, *N*, caused by possible deviation in pressure and/or temperature between proving and duty operation [-],

$E_{angle,\Delta}$: relative combined standard uncertainty of the estimate $\hat{q}_v$, due to uncertainty of the inclination angles of the *N* acoustic paths, $\hat{\phi}_i$, *i* = 1, …, *N*, caused by possible deviation in pressure and/or temperature between proving and duty operation [-],

## ACKNOWLEDGEMENTS

The *Handbook* is being worked out on an initiative from the Norwegian Society of Oil and Gas Metering (NFOGM) and the Norwegian Petroleum Directorate (NPD), and the work is supported by these institutions in a cooperation with Tekna. The authors wish to acknowledge the technical reference group of the project, consisting of (in arbitrary order) Trond Folkestad (StatoilHydro), Endre Jacobsen (StatoilHydro), Frode Flåten (ConocoPhillips), Jostein Eide (National Institute of Technology), Reidar Sakariassen (MetroPartner), Steinar Vervik (NPD), and Skule Smørgrav (FMC Technologies).

## REFERENCES

[1] **Lunde, P. and Frøysa, K.-E.:** "Handbook of uncertainty calculations. Ultrasonic fiscal oil metering stations". Handbook being prepared on behalf of the Norwegian Society of Oil and Gas Measurement (NFOGM), the Norwegian Petroleum Directorate (NPD) and Tekna. (In preparation.) (Free download will be available from www.nfogm.no.)

[2] **ISO**, "Guide to the expression of uncertainty in measurement. First edition". ISO, Geneva, Switzerland (1995).

[3] **ISO 5168:2005,** "Measurement of fluid flow – Procedures for the evaluation of uncertainties", ISO, Geneva, Switzerland (2005).

[4] **NPD**, "Regulations relating to measurement of petroleum for fiscal purposes and for calculation of $CO_2$ tax", Norwegian Petroleum Directorate, Stavanger, Norway (November 1, 2001), with (a) changes effective from January 1, 2004, and (b) changes dated August 22, 2006 (related to implementation of the EU "measurement instrument directive" (MID) [7]).

[5] **NORSOK I-105**, "Fiscal measurement systems for hydrocarbon liquid", NORSOK Standard I-105, Edition 3, Standards Norway, Oslo, Norway (August 2007).

[6] "Manual of petroleum measurement standards. Chapter 5 – Metering. Section 8 – Measurement of liquid hydrocarbons by ultrasonic flow meters using transit-time technology", 1st edition, American Petroleum Institute, Washington, U.S.A. (February 2005).

[7] "Directive 2004/22/EC of the European Parliament and of the Council of March 31 2004 on measuring instruments", Official Journal of the European Union (April 30, 2004). Effective from October 30, 2006.

[8] **Lunde, P. and Frøysa, K.-E.:** "Handbook of uncertainty calculations. Ultrasonic fiscal gas metering stations". Handbook prepared on behalf of the Norwegian Society of Oil and Gas Measurement (NFOGM) and the Norwegian Petroleum Directorate (NPD) (December 2001), 279 p. (ISBN 82-566-1009-3). (Free download available from www.nfogm.no.)

[9] **Lunde, P., Frøysa, K.-E., Neumann, S. and Halvorsen, E.:** "Handbook of uncertainty calculations. Ultrasonic fiscal gas metering stations". Proc. of the *20th North Sea Flow Measurement Workshop,* St. Andrews Bay, Scotland, 22-25 October 2002. 15 p.

[10] **Dahl, E. O., Frøysa, K.-E. and Lunde, P.:** "Handbook of uncertainty calculations. Fiscal orifice gas and turbine oil metering stations". Handbook prepared on behalf of the Norwegian Society for Oil and Gas Measurement (NFOGM), the Norwegian Petroleum Directorate (NPD) and the Norwegian Society of Chartered Engineers (NIF). ISBN 82-91341-62-1 (May 2003).

[11] "Altosonic V, Technical Datasheet. 5-beam ultrasonic flowmeter for custody transfer or liquid hydrocarbons", Krohne Altometer B.V., Dordrecht, the Netherlands. Downloaded from Krohne web site http://www.krohne-downloadcenter.com/dlc/TD_ALTOSONIC_V_en_060424.pdf (September 2008).

[12] "Caldon LEFM 240C / 240 Ci Ultrasonic meter", Sales brochure, Cameron, USA. Downloaded from web site http://www.c-a-m.com/content/products/product_detail.cfm?pid=51777 (September 2008).

[13] "Smith Meter Ultra[6] Ultrasonic Liquid Flowmeter Specifications", Bulletin SSLS001 Issue/Rev. 0.1 (10/07), FMC Technologies. Downloaded from FMC Technologies web site http://info.smithmeter.com/literature/docs/ssls001.pdf (September 2008).

[14] "Daniel Model 3804 Ultrasonic Liquid Flowmeter", Product data sheet, June 2008, Emerson Process Management, USA. Downloaded from Emerson web site http://www.emersonprocess.com/daniel/products/liquid/usonic/Model%203804%20Liquid%20Ultrasonic/Ds_Sheets/Liq_USM_DS.pdf (September 2008).

[15] **Lygre, A., Lunde, P., Bø, R. and Vestrheim, M.,** "High-precisison ultrasonic gas flowmeter. Sensitivity study. Volumes I and II." CMR Report no. 871429-1, Christian Michelsen Research AS, Bergen (March 1988). (Confidential.)

[16] **Lunde, P., Frøysa, K.-E. and Vestrheim, M.:** "*FMUSIK* - Version 1.0. Uncertainty model for the 6-path FMU 700 ultrasonic gas flow meter". CMR Report No. CMR-95-F10033, Christian Michelsen Research AS, Bergen (December 1995). (Confidential.)

[17] **ISO,** "Measurement of fluid flow in closed cirquits - Methods using transit time ultrasonic flowmeters". ISO Technical Report ISO/TR 12765:1997, ISO, Geneva, Switzerland (1997).

[18] **Lunde, P., Frøysa, K.-E. and Vestrheim, M.:** "*GARUSO* Version 1.0. Uncertainty model for multipath ultrasonic transit time gas flow meters", CMR Report no. CMR-97-A10014, Christian Michelsen Research AS, Bergen (September 1997).

[19] "GERG project on ultrasonic gas flow meters, Phase II", edited by Lunde, P., Frøysa, K.-E. and Vestrheim, M., GERG TM11 2000, Groupe Européen de Recherches Gazières (VDI Verlag, Düsseldorf, 2000).

[20] **Rosemount**, "Model 3051 Pressure Transmitter, Product Data Sheet 00813-0100-4001, Rev. DA", Rosemount Inc., Chanhassen, MN, U.S.A. (2002).

[21] **Rosemount**, "Model 3144 Temperature Transmitter, Product Data Sheet 00813-0100-4021, Rev. AA", Rosemount Inc., Chanhassen, MN, U.S.A. (2002).

[22] **Solartron,** "7835 Liquid Density Transducer. Technical Manual 7835 5001", Solartron Mobrey Limited, Slough Berks, UK (2000).

[23] **AGA-9**, "Measurement of gas by ultrasonic meters", A.G.A. Report no. 9, American Gas Association, Transmission Measurement Committee (June 1998).

[24] **OIML,** "Rotary piston gas meters and turbine gas meters", OIML Recommendation No. 32, International Organization of Legal Metrology, Paris, France (1989).

North Sea FLOW Measurement Workshop

# Paper 8.3

# Thermal Lagging – The Impact on Temperature Measurement


***Sarah Kimpton***
***Advantica Ltd***

***Ali Niaza***
***Advantica Ltd***


TÜV SÜD

nel technology for life

# Thermal Lagging – The Impact on Temperature Measurement

**Sarah Kimpton, Advantica Ltd**
**Ali Niazi, Advantica Ltd**

## 1 INTRODUCTION

Large custody transfer/fiscal metering systems in the United Kingdom are regularly audited to ensure compliance with best industry practice and British and international standards. One recurrent finding from these audits has concerned the lack of thermal lagging on both the upstream and downstream lengths as well as the impulse lines connecting the primary device to the pressure and differential pressure transmitters. Typical findings from recent audits are:

> *The orifice fittings, meter tube upstream and downstream straight lengths and temperature fittings are not thermally insulated and are open to the elements in an exposed location*
>
> *In an exposed site location, an even heat transfer throughout the metering tube lengths cannot be guaranteed and it is possible to introduce temperature gradients within a flowing stream. There may be a big difference between the flowing gas temperature and the ambient temperature depending on the time of the year*
>
> *The exposed position of the meter run and the lack of lagging on the pipe work and the temperature probe and fitting means that the temperature used to calculate gas density is unlikely to reflect the true flowing gas temperature*.

The standards and best practice documents recommend that the temperature sensor is placed in a thermowell which is then inserted into the gas stream of the flowing gas. The auditors claim that if there were no lagging, then the temperature measured in a thermowell may not be the same as the gas temperature. A temperature difference of 0.5 ºC will impact on volume measurement by as much as 0.3%.

For fiscal/custody transfer metering systems, the temperature is always measured downstream of the primary device, regardless of the type of the meter, unless it can be demonstrated that alternative techniques can provide similar performance. For orifice plates, the temperature is measured between five and fifteen diameters downstream of the orifice plate. For turbine and ultrasonic meters, the temperature is measured as close to the meter as possible, approximately five diameters downstream.
The majority of natural-gas metering-systems in the United Kingdom were built in the 1970s and 1980s with no thermal insulation to protect the temperature measurement from ambient variations. It was thought that the impact of the ambient temperature on the temperature of the flowing gas was so small that it could be neglected. Historically the belief was that if the meters were larger than 8” (200 mm), then lagging was unnecessary.

Advantica were requested as an independent organisation to investigate the impact of lagging on temperature measurement. This paper addresses the historical work carried out in this area, examines the previous experimental measurements and presents new results from a computational fluid dynamics mathematical model.

## 2 RECOMMENDATIONS FROM STANDARDS

The recommendations for lagging in ISO 5167 and IGE/GM/1 are given below.

There are references to the effect of ambient temperature on the gas temperature in the Institute of Gas Engineers Gas Measurement Procedure IGE/GM/1[1]. Paragraph 4.3.2.2 states:

*Gas temperature variations at a meter will be affected by the proximity of gas heaters, the Joule-Thomson cooling effect caused by large pressure reductions and the exchange of heat between the gas and the environment. In the absence of heaters and large pressure reduction equipment at above-ground meter installations being fed from underground pipe, the gas temperature will tend to follow ambient at low flows and pressure, whereas at high flow and pressure it will follow ground temperature.*

Paragraph 5.10.1.6 concerns meter installation pipe work. A note on thermowells states the following:

*Note: In order to ensure that the measured temperature at the thermowells is the same as that of the gas passing through the meter, it may be necessary to lag the external part of the thermowell and the pipe work for a suitable distance upstream and downstream of the meter.*

ISO 5167 is the standard concerned with orifice-plate metering. In both the 1991[2] and the 1997[3] versions under *Installation Requirements*, paragraph 7.1.9 states:

*The pipe and the pipe flanges shall be lagged. It is however, unnecessary to lag the pipe when the temperature of the fluid, between the inlet section of the minimum straight length of the upstream pipe and the outlet of the minimum straight length of the downstream pipe, does not exceed any limiting value for the accuracy of flow measurement required.*

The 2003[4] version of ISO 5167 paragraph 7.1.7 states:

*Insulation of the meter may be required in the case of temperature differences between the ambient temperature and the temperature of the flowing fluid which are significant given the uncertainty of measurement required. This is particularly true in the case of fluids being metered near their critical point where small temperature changes result in major density changes. It can be important at low flow rates where small temperature changes result in major density changes. It can be important at low flow rates, where heat transfer effects may cause distorted temperature profiles, for example, stratification of temperature layers from top to bottom. There may also be a change in the mean temperature value from the upstream to the downstream side of the meter run.*

## 3 HISTORICAL WORK

There have been a number of theoretical and experimental investigations into temperature measurement at the British Gas Engineering Research Station (later to become part of Advantica). Some significant results are listed below.

### 3.1 Thermowell Fatigue Failure Investigation

Pallan and Wood[5] investigated thermowell fractures due to vibration at Bacton Terminal and Alrewas Compressor Stations. As part of the work, the authors investigated the feasibility of measuring temperature on the surface of the pipe under normal and extreme conditions, both with and without thermal insulation.

Theoretical calculations were carried out to investigate the temperature profile across an unlagged 24” (600 mm) diameter pipe with a 0.5” (12.5 mm) wall thickness. Three sets of calculations were carried out:

- At typical ambient conditions of 10 ºC with a 3 m/s cross wind and with a gas flow of 8.5 mscmd at 15.56 ºC and 55 bar. The temperature of the outside of the pipe wall was 15.43 ºC and the temperature of the inside of the pipe wall was 15.45 ºC

- At severe ambient conditions of -1 ºC with a cross wind of 10.7 m/s and with a gas flow of 14 mscmd at 68 bar and 37.8 ºC. The temperature of the outside of the pipe wall was 36.19 ºC and the temperature of the inside of the pipe wall was 36.51 ºC.

- At the same severe ambient conditions with a gas flow of 14 mscmd at 68 bar and 37.8 ºC, the pipe was covered with 1“ of lagging. The temperature of the outside of the pipe wall was 37.71 ºC and the temperature of the inside of the pipe wall was 37.72 ºC.

The temperature measuring error from a thermowell may be considered to comprise several sources. The main ones are conduction error, kinetic energy error, radiation error, intrinsic dynamic error and gradient error. Theoretical analyses of the main sources of temperature measurement error of a thermowell indicated that the conduction error was the only one that could significantly affect the performance of a temperature measurement in a thermowell.

At Low Thornley test site, experiments were carried out on an 8” unlagged thermowell designed to an old ERS drawing EW 21. The thermowell was subjected to an artificial ambient temperature range by surrounding the thermowell flange with a water bath; temperatures of 39 ºC below ambient and 28 ºC above ambient were achieved. Gas velocities of up to 20 m/s were obtained. The gas temperature was measured by placing a thermocouple in the gas stream; this was compared with another thermocouple placed in the thermowell.

The results from these tests showed that the temperatures sensed in the thermowell were within ±1.7 ºC over the range of 39 ºC below ambient and 28 ºC above ambient. The tests also demonstrated that the temperature readings were within ±0.5 ºC when the gas temperature was between 39 ºC below and 11 ºC above ambient.

### 3.2 Gas Temperature Inferred from Pipe Wall Temperature

Following the fracture and failure of thermowells at compressor stations and elsewhere, Pallan[6] investigated the relationship between pipe-wall temperature and gas temperature. The theoretical relationship between pipe-wall temperature and gas temperature for a 24“ pipe is reproduced from Pallan’s report in figure 3.1. A number of experimental measurements were made on 6“ pipe and 24“ pipe - the surface temperatures were compared with thermowell temperatures.

For 6“ pipes, agreement of ±0.5 ºC between pipe-wall and gas temperature was measured over a temperature range of 6 to 20 ºC. For 24“ pipes, greater differences were observed, especially for low gas temperatures; between 6 and 12 ºC, differences of 0.5 to 2.5 ºC were observed whereas between 12 and 20 ºC the differences were of the order of 0 to 1 ºC. It is assumed that these measurements were for unlagged systems. The authors of this report state that under “well monitored” conditions, the difference between the wall temperature and the gas temperature was within 0.1 ºC over a seven day period.

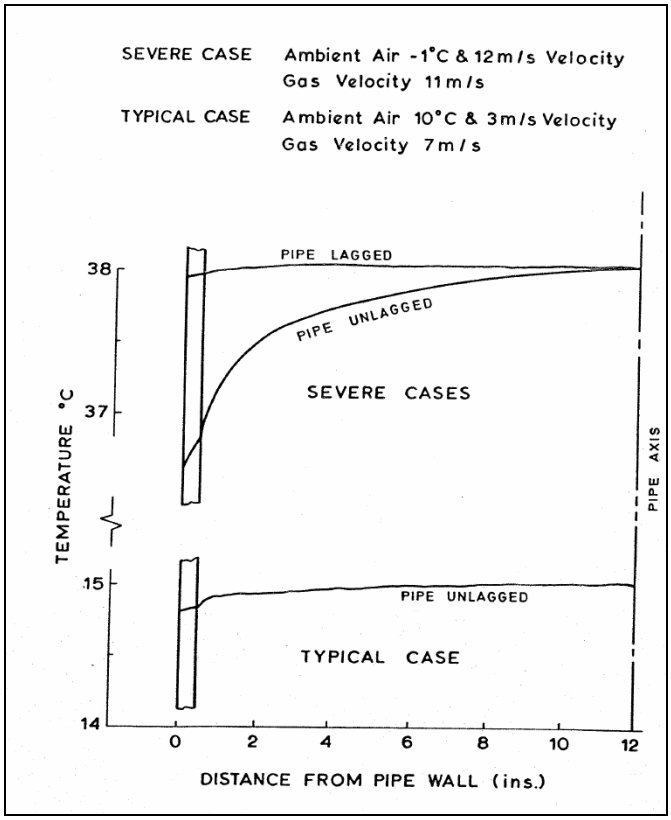


Figure 3.1 Relationship between pipe-wall temperature and gas temperature for a 24“ pipe

### 3.3 Surface-Temperature Measurement at Compressor Stations

Fenwick[7] carried out theoretical and experimental work to establish the principles of inferring gas temperature from the temperature of the outside pipe surface. The surface pipe-temperature is dependent on:

- Ambient temperature
- Gas temperature
- Gas density
- Gas velocity
- Speed of the wind impinging on the pipe
- Solar radiation
- Pipe wall thickness

Theoretically, for a steady gas temperature, the temperature difference between the outside wall of the pipe and the gas will not exceed 0.6 ºC if:

- gas velocity is in excess of 6.1 m/s
- gas pressure is greater than 38 bar
- ambient to gas temperature difference is less than 40 ºC
- wind speed is not greater than 1.2 m/s.

Variation in pipe wall thickness has very little effect due to the good thermal conductivity of steel. The speed of the wind blowing across a pipe has a marked effect on the accuracy of measurement. If the wind speed in the above example were 6.1 m/s, the temperature difference between the gas and the pipe surface would be 2 ºC.

The calculations above assumed that there was no lagging present. The use of lagging will extend the range within which the pipe surface temperature can be used by reducing the effects of wind and solar radiation. For example, if a surface-mounted temperature sensor

were covered with a 12.5 mm thick pad of lagging that extended 0.254 m either side of the sensor, the measured temperature should be within 0.1 ºC of the true temperature even though the exposed pipe wall were 50 ºC above or below the gas temperature.

To test the theoretical calculations, experiments were carried out at two compressor stations under normal running conditions. The temperature at the surface of the pipe was compared with the temperature measured in the thermowell. At steady running conditions with no extreme gas temperature changes, the maximum measured temperature difference between the gas and the pipe surface was 0.2 ºC at a gas velocity of about 9.1 m/s.

### 3.4 Surface Temperature Response Times and Effects of Removing Thermal Insulation on Surface Temperature Measurement

Ingram[8] compared the response time of a surface-mounted temperature measurement with that from within a thermowell. Both thermometers were insulated. The surface-temperature sensor was surrounded with a 50 mm layer of insulation that extended round the full circumference of the pipe for a length of one pipe diameter. The thermowell was insulated over a radius of 300 mm around the flange. The tests were carried out over two flow-rate ranges – a low flow-rate change (11.7 to 8.7 mscmd) and a high flow-rate range (18.3 to 15.7 mscmd). The surface temperature measurement agreed with the thermowell temperature measurement to within ±0.1 ºC.

Ingram[9] also investigated the effectiveness of thermal insulation on surface-mounted temperature sensors. The temperature measured by three surface-mounted sensors was compared with the temperature determined by two sensors, each of which was in a lagged thermowell. Under stable thermal conditions, a set of temperature data was recorded from the lagged surface-mounted sensors and the lagged thermowell sensors. The lagging on the surface-mounted sensors was then removed and the measured temperature compared with that of the sensors in the thermowells. The ambient air temperature during the tests was 12.5 ºC with a light breeze. The gas temperature was about 6 ºC.

Before the lagging was removed from the surface-mounted sensors, the thermowell and surface-mounted sensor recorded temperatures that agreed to 0.17 ºC. When the lagging was removed, the average difference was 1.20 ºC.

The insulation used during these tests was local to the temperature measurement only. The lagging around the thermowell extended over a radius of 200 mm around the flange. The lagging on the surface-mounted sensors extended around the full circumference of the pipe and for a length of one pipe diameter either side.

Ingram stressed that it is important for thermal insulation to be waterproofed. When the gas temperature is lower than ambient temperature, airborne moisture condenses on the unprotected pipe surfaces which can be absorbed by unprotected insulation. The insulating properties of commonly used lagging materials, such as fibre glass or rock wool, are greatly reduced once water has been absorbed.

### 3.5 St Fergus Plant Aftercooler Temperature Measurement

Ingram[10] studied the effect of lagging on short (64 mm) thermowells at St Fergus compressor station. Due to fracture problems with long thermowells, short thermowells were fitted that did not protrude within the gas flow. The platinum-resistance-thermometer element was therefore not in the gas flow but level with the pipe wall in the neck flange. Discrepancies in the gas temperature measurement were resolved by lagging the short thermowells and agreement of better than ±1 ºC was achieved.

The 64 mm thermowell measurements, however, had very long response times of about 30 minutes which was unacceptable. Acceptable alternatives were either to install lagged surface-mounted temperature sensors or 226 mm (8.9“) thermowells.

### 3.5 Assessment of Gas Temperature Measurement Systems at Churchover Compressor Station

Nisbet and Robertson[11] compared surface-mounted temperature sensors with platinum resistance thermometers in direct contact with the gas and supported at varying radial depths into the gas stream.
The surface-mounted sensors were platinum resistance thermometers spirally wound in a ceramic support 25 mm long by 4 mm diameter mounted in a brass housing. The housing was bonded on to the outside of the pipe by a silicon rubber adhesive. Four sensors were located around the outside diameter of the pipe.

The sensors in the gas were also platinum resistance-thermometers comprising a spiral element wound on a cylindrical grooved ceramic support mounted in a probe. Four sensors were mounted on the probe at varying depths (see figure 3.2). The probe was inserted into the gas stream via a 2“ flanged stabbing. The insertion depths were 13, 140 and 267 mm; one further sensor was fitted 50 mm above the pipe inner wall (within the neck of the flange but outside the gas stream).

The surface sensors, and the stabbing and the flange and emergent fittings of the profile probe were comprehensively lagged. The mass flow of the gas through the system varied between 150 and 200 kg/s.

The gas temperature measurements covered only a limited range of 20.9 to 24.7 ºC. However, the maximum difference between the surface measurement and the insertion measurement was 0.15 ºC. The maximum temperature difference across the pipe profile was within the measurement uncertainty of ±0.03 ºC. The sensor located 50 mm outside the inner pipe wall was up to 0.15 ºC different to the temperature measured by the sensors within the gas stream.

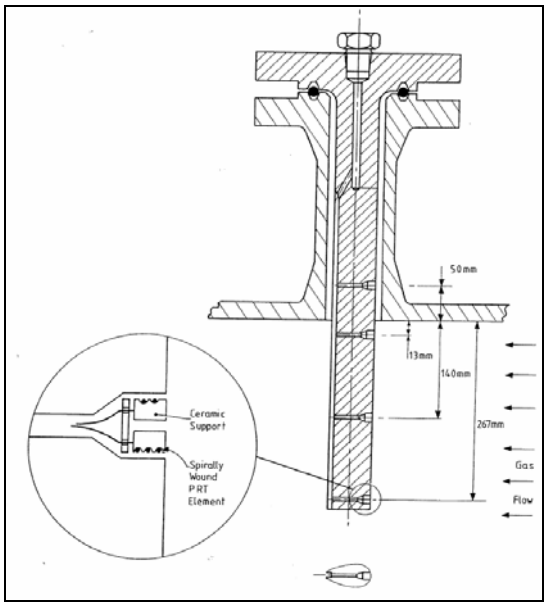


Figure 3.2 Temperature measurement insertion probe showing positions of PRTs

### 3.6 Thermowell Temperature sensor

It is important that a thermometer in the thermowell is at the gas temperature. Good thermal coupling between the thermometer and the thermowell is important. This can be achieved by ensuring that the bottom of the thermowell is filled with a suitable low-vapour-pressure heat-conducting fluid to optimise response times. It is also necessary to ensure that the bore of the thermowell matches the measuring element – sometimes an insert is required to ensure good thermal contact.

# 4 COMPUTATIONAL FLUID DYNAMICS

A study has been commissioned from Prof W Malalasekera of Loughborough University[12] to investigate heat transfer in thermowell installations using CFD. Prof Malalasekera is a recognised authority on CFD; for example, he has co-authored a textbook for advanced undergraduate and postgraduate students studying CFD and numerical methods[13].

## 4.1 Details of the CFD Model

Prof Malalasekera undertook a numerical study of the heat transfer characteristics of thermowells in natural gas pipelines. He modelled a thermowell that was mounted on a connecting flange attached to the pipe. The thermowell protruded into the pipe by 90 mm and it was exposed to the gas flow. A temperature sensing probe was placed inside the thermowell (but not exposed to the gas) to measure the gas temperature. The flange and the pipe line were exposed to ambient conditions which could vary considerably. There was some concern that there could be heat transfer between the ambient air and the flange and the thermowell body such that the temperature measured by the thermometer may not be the same as the gas temperature.

In this work, the temperature distribution inside the thermowell was determined using *CFD* to calculate the heat flow and conjugate transfer in the flange/thermowell arrangement. A range of ambient conditions was considered to investigate the effect on the temperature distribution inside the thermowell. The calculations were done both with and without thermal insulation.

## 4.2 Geometry of the Thermowell

Thermowells are typically installed in a pipe line using a flange arrangement as shown in figure 4.1. The analysis of heat transfer was considered for two gas pipe diameters, 24” (610 mm) and 8” (219.1 mm). In both cases a 90 mm length section of the thermowell was considered to be inside the pipe.

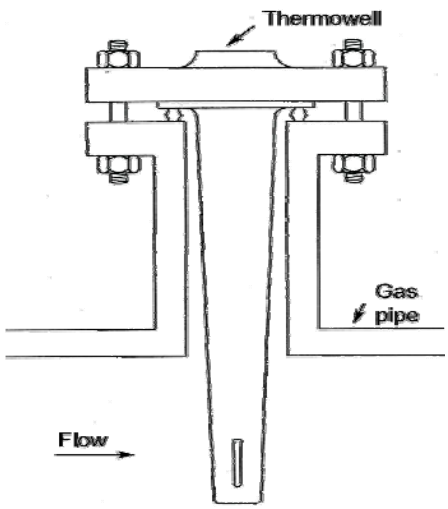


Figure 4.1 Schematic of a typical thermowell installation

## 4.3 Operating and Ambient Conditions

Two pipeline operating conditions were considered:

- Gas flowing at a temperature of 37.7 °C and a pressure of 60 bar.

- Gas flowing at a temperature of 15 °C and a pressure of 60 bar.
- Various winter and summer ambient conditions were also considered:
- Winter temperatures of 0, -5 and -10 °C with wind speeds of 5 m/s
- Summer temperatures of 30 and 35 °C with a wind speed of 1 m/s

For summer weather conditions, direct solar gains on the pipe surfaces were taken into account using data from the *Chartered Institute of Building Services Engineers*. A table summarising the conditions used by Prof Malalasekera is shown in table 4.1.

The *Case ID* relates to the calculation conditions:

- *HT* denotes gas temperatures of 37.7 °C
- *LT* denotes gas temperatures of 15 °C
- *24* or *08* denote 24“ or 8“ pipe diameters respectively
- *W1, W2 and W3* denote winter temperatures of 0, -5 and -10 °C respectively
- *S1* and *S2* denote summer temperatures of 30 and 35 °C respectively

Gas properties, such as mass density, gas velocity and viscosity, were provided by Advantica. Heat-transfer coefficients of the steel pipe work in the summer and winter ambient conditions were calculated using data from the *American Petroleum Institute.* The pipe walls were treated to be smooth and standard roughness conditions were used.

| Run no. | Case ID | Pipe diameter (mm) | Flow velocity (m/s) | Gas temperature (°C) | Ambient temperature (°C) |
|---|---|---|---|---|---|
| 1 | HT24W1 | 610.0 | 10.035 | 37.7 | 0.0 |
| 2 | HT24W2 | 610.0 | 10.035 | 37.7 | -5.0 |
| 3 | HT24W3 | 610.0 | 10.035 | 37.7 | -10.0 |
| 4 | HT24S1 | 610.0 | 10.035 | 37.7 | 30.0 |
| 5 | HT24S2 | 610.0 | 10.035 | 37.7 | 35.0 |
| 6 | LT24W1 | 610.0 | 8.867 | 15.0 | 0.0 |
| 7 | LT24W2 | 610.0 | 8.867 | 15.0 | -5.0 |
| 8 | LT24W3 | 610.0 | 8.867 | 15.0 | -10.0 |
| 9 | LT24S2 | 610.0 | 8.867 | 15.0 | 30.0 |
| 10 | LT24S2 | 610.0 | 8.867 | 15.0 | 35.0 |
| 11 | HT08W1 | 219.1 | 14.278 | 37.7 | 0.0 |
| 12 | HT08W2 | 219.1 | 14.278 | 37.7 | -5.0 |
| 13 | HT08W3 | 219.1 | 14.278 | 37.7 | -10.0 |
| 14 | HT08S1 | 219.1 | 14.278 | 37.7 | 30.0 |
| 15 | HT08S2 | 219.1 | 14.278 | 37.7 | 35.0 |
| 16 | LT08W1 | 219.1 | 13.412 | 15.0 | 0.0 |
| 17 | LT08W2 | 219.1 | 13.412 | 15.0 | -5.0 |
| 18 | LT08W3 | 219.1 | 13.412 | 15.0 | -10.0 |
| 19 | LT08S1 | 219.1 | 13.412 | 15.0 | 30.0 |
| 20 | LT08S2 | 219.1 | 13.412 | 15.0 | 35.0 |

Table 4.1 Summary of the calculation conditions

### 4.4 The CFD Model

The CFD model treated the investigation as a conjugate heat transfer problem; that is, the equations governing the conductive heat transfer in the solid parts were solved simultaneously with the fluid flow equations. In this way, the temperature distribution of both the natural gas and the pipe work was determined. The model considered a 700 mm length of pipe which incorporated the thermowell and its flanges.

The three-dimensional geometry had a number of complex features in the thermowell area. A tetrahedral mesh with varying grid densities was best suited for this kind of geometry. Figure 4.2 shows the cross section of a typical grid. The darker areas indicate a more concentrated grid in the flange and thermowell area to accommodate all the geometrical features as well as to obtain a refined and more resolved temperature distribution. A typical grid consisted of more than 550,000 elements. The larger models that included insulation and longer pipe lengths consisted of more than 760,000 elements.

Figure 4.2 A typical grid used for the CFD modelling of a thermowell

### 4.5 Results of Gas Velocity Calculations

The gas velocity around the thermowell was modelled at a number of conditions but the results were similar – an example is shown in figure 4.3 for a 24” pipe. The colour code ranges from blue (low flow) through green and yellow and finally to red (high flow). It can be seen that the flow wraps round the thermowell surface and recombines afterwards. There is a small amount of flow in the gap between the thermowell surface and the stabbing; the flow appears to be stagnant in this region as the space available is restricted.

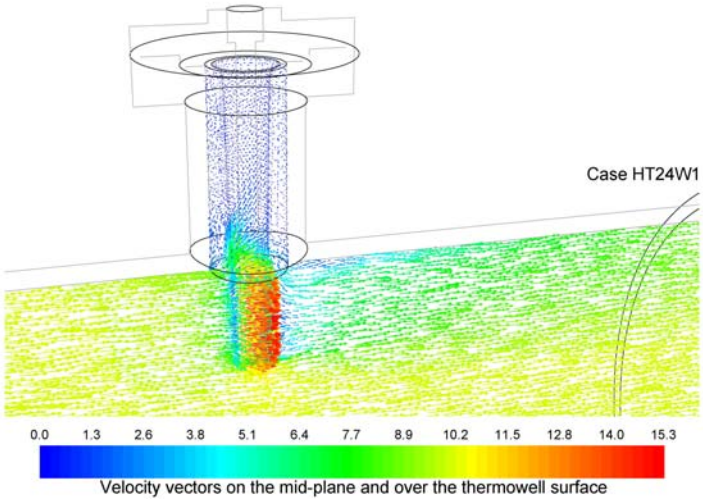


Figure 4.3 Velocity distribution in the mid-plane and gas-side surface of the thermowell.

### 4.6 Results of Temperature Simulations for Unlagged 24" Pipe

Prof Malalasekera provided results for all the cases listed in table 4.1. A sample of results with the most extreme difference between ambient and gas temperature is shown here – these are cases HT24W3, HT24S2, LT24W3, and LT24S2.

Figure 4.4 shows the temperature distribution when ambient temperature was -10 °C and the gas temperature was 37.7 °C. The temperature of the flange area and the top part of the thermowell stabbing was less than the gas temperature but it is clear that the bottom of the thermowell remained at the gas temperature. The temperature measurement at the bottom of the thermowell did represent the gas temperature.

Figure 4.5 shows the temperature distribution for summer conditions (ambient temperature is 35 °C). The solar gain was included in the simulations. In this case the blue colour indicated a temperature close to the gas temperature (37.7 °C) and the red indicated higher temperatures. It is interesting to note that there was an increase of temperature in the exposed part of the flanges and the thermowell. Further inspection indicated that the pipe work walls were at a slightly higher temperature (close to 40 °C) than the gas. The bottom of the thermowell was, however, still at the gas temperature and temperature measurement were unaffected by the ambient conditions.

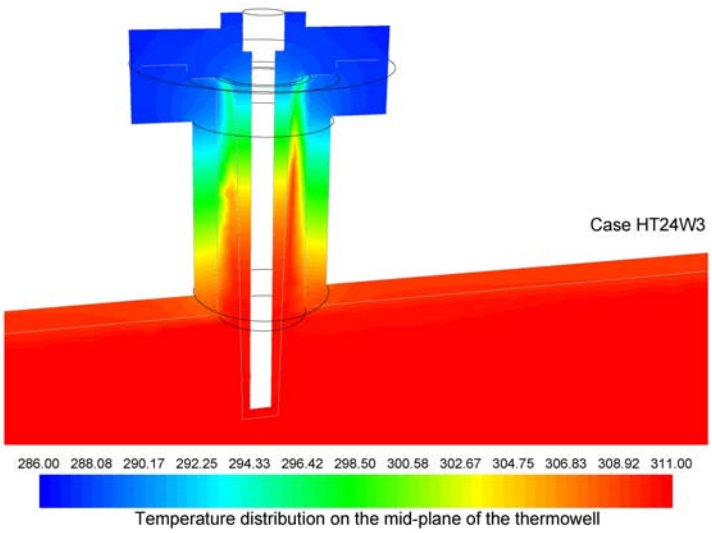

Figure 4.4. Temperature distribution in a 24" pipe for a gas temperature of 37.7 °C and ambient temperature of -10 °C. The temperature scale is in kelvin – the blue is 13 °C and the red is 38 °C.

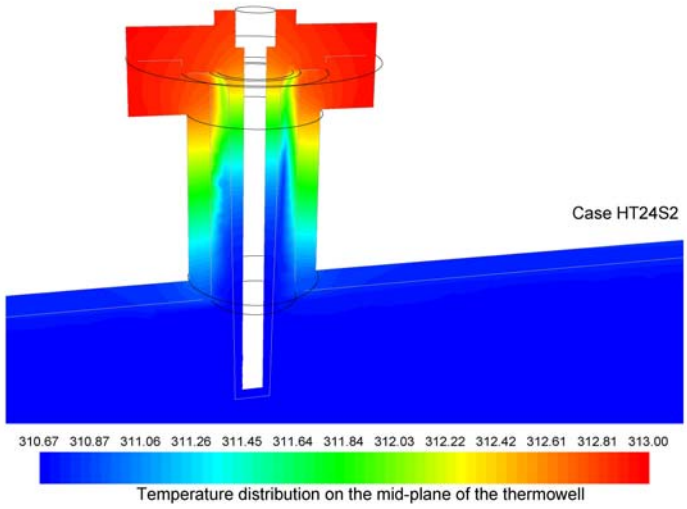


Figure 4.5. Temperature distribution in a 24" pipe for a gas temperature of 37.7 °C and ambient temperature of 35 °C. The temperature scale is in kelvin – the blue is 37.5 °C and the red is 40 °C.

Figure 4.6 shows the temperature distribution for an ambient temperature of -10 °C and a gas temperature of 15 °C. Although there was a considerable drop in the temperature of the flange, the temperature at the bottom of the thermowell remained unaffected.

Figure 4.7 shows the temperature distribution for summer conditions of 35 °C. There was a notable increase in temperature around the flange but the bottom of the thermowell remained at the gas temperature of 15 °C.

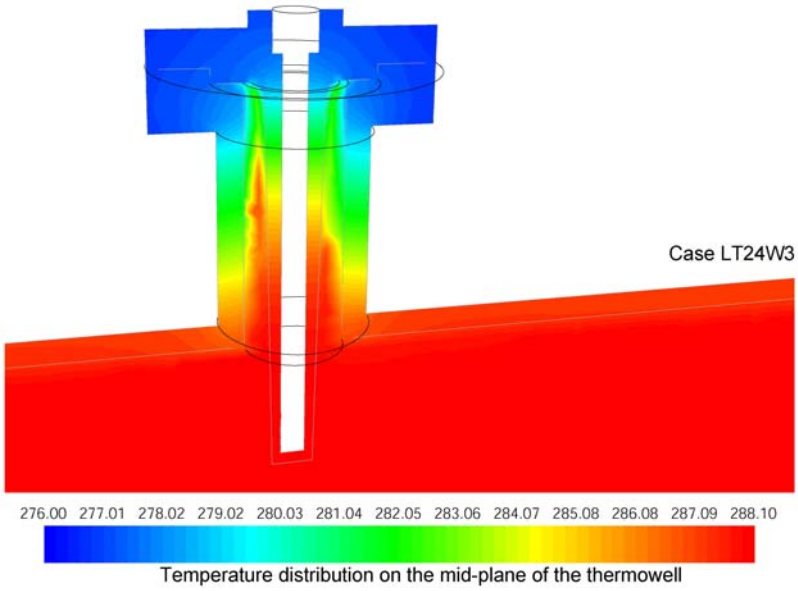


Figure 4.6 Temperature distribution in a 24" pipe for a gas temperature of 15°C and ambient temperature of -10 °C. The temperature scale is in kelvin – the dark blue corresponds to 3 °C and the red to 15 °C.

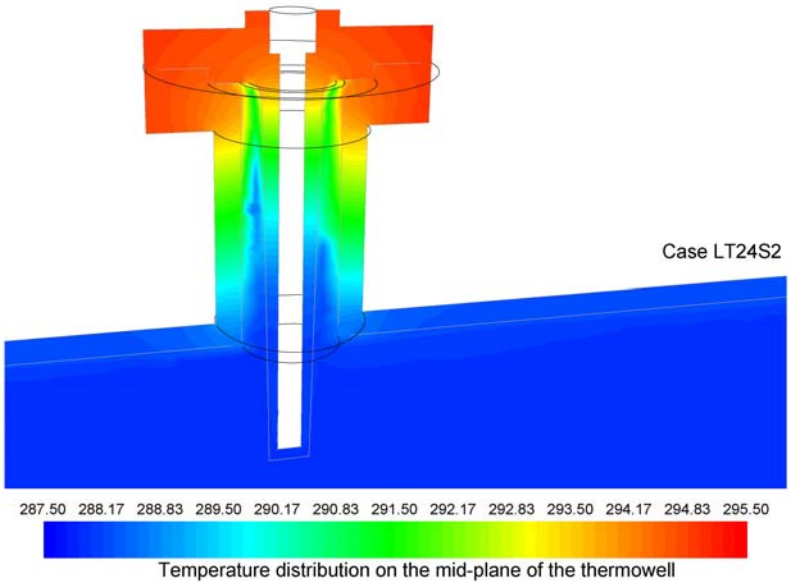


Figure 4.7. Temperature distribution in a 24" pipe for a gas temperature of 15 °C and ambient temperature of 35 °C. The temperature scale is in kelvin – the dark blue corresponds to 15 °C and the red to 23 °C.

### 4.7 Results of Temperature Simulations for Unlagged 8" Pipe

The general flow pattern across the thermowell was similar to that for the 24" pipe. However, for this pipe diameter, the wall was thinner and there was slightly more space between the pipe stabbing wall and the gas side of the thermowell surface. The gas velocity around the thermowell was therefore greater than that for the 24" pipe.

Figure 4.8 shows the temperature distribution for an ambient temperature of -10 °C and a gas temperature of 37.7 °C. The temperature of the flange and the top of the thermowell was much cooler than the gas as indicated by the dark blue. However, the bottom of the thermowell remained at the gas temperature.

Figure 4.9 shows the temperature predictions for summer conditions of 35 °C and a gas temperature of 37.7 °C. The ambient temperature increased the temperature in the flange area which was indicated by the red. However, the bottom of the thermowell was seen to be at gas temperature.

Figure 4.10 shows the temperature distribution when the gas temperature was 15 °C and the ambient temperature was -10 °C. Although there was a considerable decrease in the temperature of the flange area, the temperature at the bottom of the thermowell remained unaffected at 15 °C.

Figure 4.11 shows the temperature distribution for an ambient temperature of 35 °C and a gas temperature of 15 °C. The figure shows that there was a considerable increase in temperature around the flange but the bottom of the thermowell remained at 15 °C.

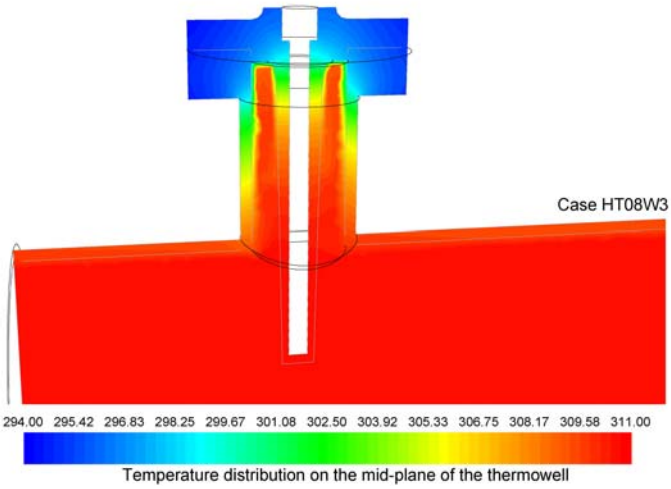


Figure 4.8 Temperature distribution in a 8" pipe for a gas temperature of 37.7 °C and ambient temperature of -10 °C. The temperature scale is in kelvin – the dark blue corresponds to 21 °C and the red to 38 °C.

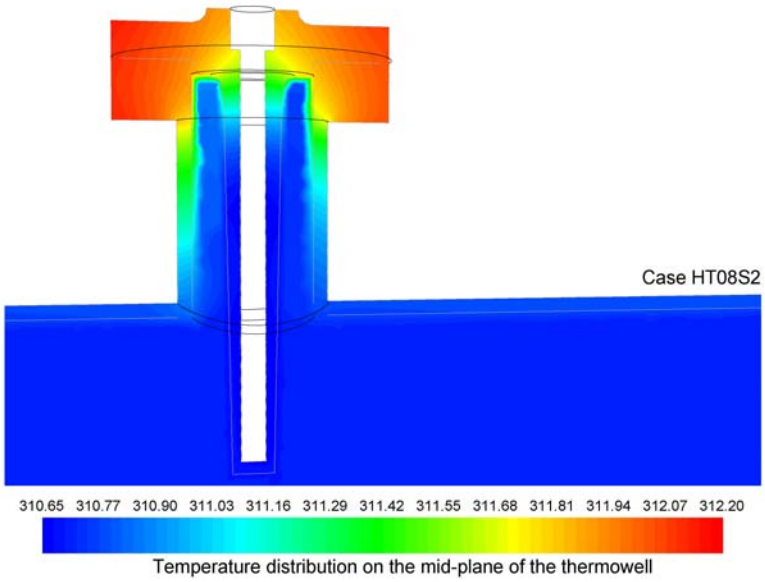


Figure 4.9 Temperature distribution in a 8" pipe for a gas temperature of 37.7 °C and ambient temperature of 35 °C. The temperature scale is in kelvin – the dark blue corresponds to 37.5 °C and the red to 39 °C

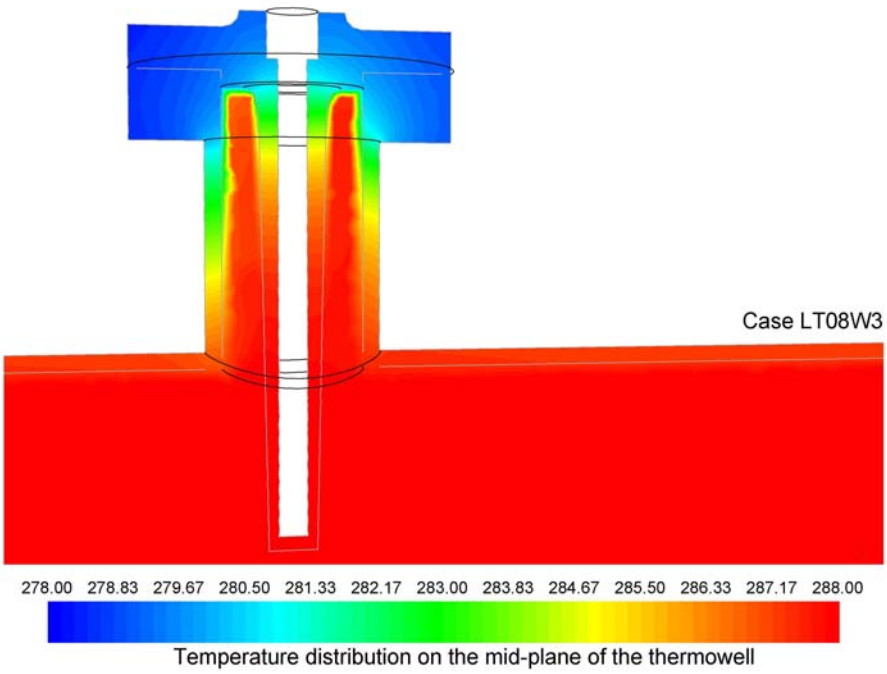


Figure 4.10 Temperature distribution in a 8" pipe for a gas temperature of 15 °C and ambient temperature of -10 °C. The temperature scale is in kelvin – the dark blue corresponds to 5 °C and the red to 15 °C

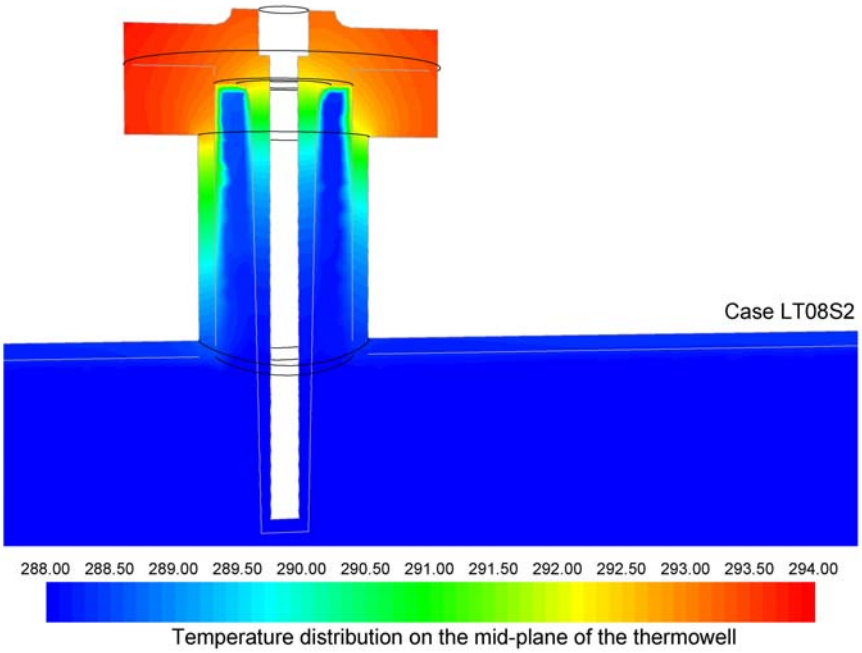


Figure 4.11 Temperature distribution in a 8" pipe for a gas temperature of 15 °C and ambient temperature of 35 °C. The temperature scale is in kelvin – the dark blue corresponds to 15 °C and the red to 21 °C

### 4.8 Temperature Simulation Results for Insulated Thermowells

Simulations were also presented for insulated thermowell temperature measurements in order to compare previous work carried out by Nisbert and Robertson in this area. These experiments were designed to demonstrate that if a short part of the pipe is insulated surface mounted temperature measurement is acceptable. The insulation extended around the full circumference of the pipe and for a total length of 630 mm with the thermowell positioned midway.

Figure 4.12 and figure 4.13 show the overall temperature distribution across the mid plane through the thermowell for 24" and 8" pipe respectively. Only the exposed parts of the insulation were at the ambient temperature of -10 °C; the thermowell, flange and the insulated parts of the pipe wall surfaces were well protected from ambient conditions as shown by the red colour. The temperature distribution around the top of the thermowell was explored in detail by plotting contours in a narrow temperature range; the results indicated that there was a 2 °C variation. The majority of the thermowell and the thermowell stabbing was well protected and remained at the gas temperature.

It is worth noting that only a short section of the pipe has been considered to be insulated. It appears that a 630 mm length is more than sufficient to prevent the exposure of any part of the thermowell to ambient effects. The temperature changes at the edge of the insulation were examined closely. The simulations predicted small temperature variations in the un-insulated parts of the pipe wall (about 1.5 °C for 24" pipe and 2.5 °C for 8" pipe). However, the effect does not show any significant penetration into the insulated section which indicates that the insulation is more than adequate.

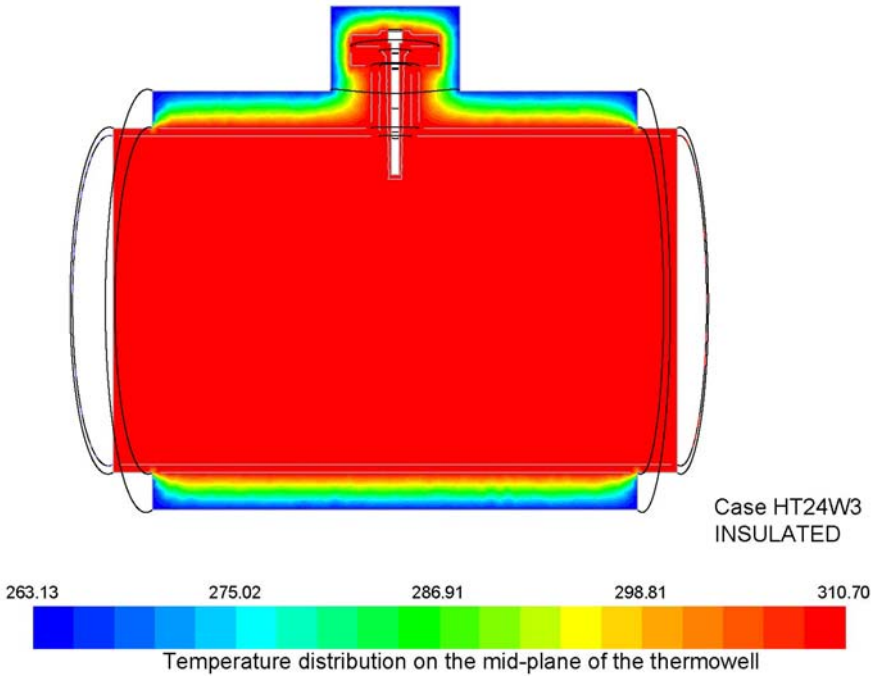


Figure 4.12. Temperature distribution for a 24" pipe insulated over a 630 mm section at the thermowell location. The gas temperature is 37 °C and ambient temperature is -10 °C. The temperature scale is in kelvin – the dark blue corresponds to -10 °C and the red to 37 °C

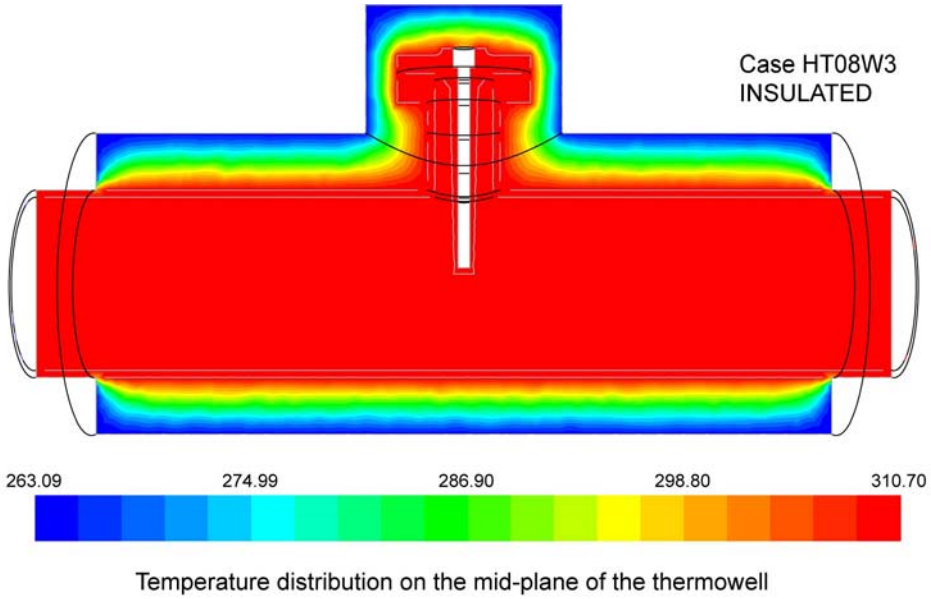


Figure 4.13 Temperature distribution for an 8" pipe insulated over a 630 mm section at the thermowell location. The gas temperature is 37 °C and ambient temperature is -10 °C. The temperature scale is in kelvin – the dark blue corresponds to -10 °C and the red to 37 °C

### 4.9 Results for Low Velocity Gas Flows

A simulation was carried out for an insulated 8" pipe when the velocity of the gas was very low (1.1 m/s). The gas temperature was 15 °C and the ambient temperature was -10 °C. The results are shown in figure 4.14. The thermowell remained at the gas temperature and, as in previous cases, small variations in temperature around the top area of the thermowell and at the edges of the insulation were present. The reduction in temperature in the top part of the thermowell and flange area was about 2 °C. The drop in wall temperature in the exposed part of the wall was about 3 °C. The edge effects did penetrate into the insulated part of pipe wall for a short distance. The thermowell is, however, not connected to the pipe wall directly and therefore not affected by the minor drop in cylinder wall temperature. The simulation clearly shows that even in this extreme case the bottom of the thermowell remains at the gas temperature.

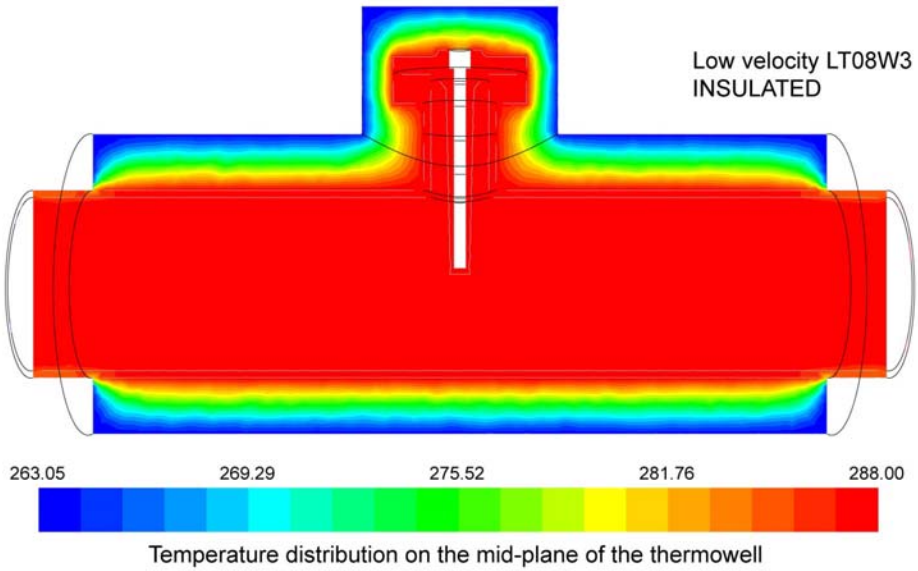


Figure 4.14. Temperature distribution for an 8" pipe insulated over a 630 mm section at the thermowell location. The gas temperature is 37 °C and ambient temperature is -10 °C. The temperature scale is in kelvin – the dark blue corresponds to -10 °C and the red to 37 °C

## 5 CONCLUSIONS

### 5.1 Experimental Measurements

The theoretical calculations of Pallan in the early 1970s indicated that the difference in the temperature of the pipe wall and the temperature of the gas were likely to be small even for unlagged pipe subjected to severe conditions. The largest source of temperature error was predicted to be from thermal conduction. Pallan's experimental measurements showed that an unlagged thermowell determined the gas temperature to within ±1.7 ºC when the ambient temperature varied between 39 ºC below and 28 ºC above the gas temperature. The tests also demonstrated that the temperature readings were within ±0.5 ºC when the gas temperature was between 39 ºC below and 11 ºC above ambient.

Theoretical calculations by Fenwick on pipe-surface temperatures show that for high gas pressures and velocities the difference between the gas temperature and the pipe surface temperature is less than 0.6 ºC. The wind speed, however, had a significant impact. Experimental measurements at two compressor stations indicated that the difference between the gas temperature measured in a thermowell and the pipe surface temperature was only 0.2 ºC. These measurements were made in an enclosed environment so the impact of wind speed was not an issue.

The experimental measurements by Ingram confirmed that the agreement between the gas temperature measured in a lagged thermowell and that measured with a lagged surface temperature sensor was within ±0.1 ºC. Ingram also looked at the effect of removing insulation from surface temperature sensors – the temperature difference between the thermowell and the surface sensor with lagging was 0.17 ºC, When the lagging was removed, the temperature difference increased to 1.2 ºC. Other points raised by Ingram were:

- The effectiveness of lagging is considerably reduced if it is not waterproofed.

- Surface-mounted temperature measurement is preferable to very short thermowells in which the sensing element is in the thermowell neck flange

Nisbert and Robertson's measurements compared surface-mounted temperature measurements with temperature measurements in a thermowell at various depths. The maximum difference between the two sets of measurements was 0.15 ºC – the greatest difference was for the sensor located within the thermowell stabbing.

### 5.2 Summary of CFD Calculations

The CFD study looked at temperature measurements in thermowells in 8" and 24" pipes transporting natural gas at 37.7 °C and 15 °C. Five different ambient conditions (0 °C, -5 °C, -10 °C, 30 °C and 35 °C) were considered. Under winter conditions, the simulations show that the temperatures around the top of the thermowell and the flange area were influenced by ambient temperature. The degree of influence increased with the decrease in ambient temperature. For summer conditions, the simulations show a considerable increase in temperature around the flange area and the top part of the thermowell. This increase is greater for the higher ambient temperature case.

Further simulations were carried out with insulation around the thermowell and the pipe surfaces. It was clear that the thermowell and the flange were adequately protected by the insulation and only a small temperature change can be seen around the top of the thermowell and flange. The edge effects at the end of the insulation section did not penetrate into the insulated section.

A simulation with low velocity gas flow in an insulated 8" pipe was also carried out. The results were similar to the other insulated cases. No significant drop in temperature in the thermowell is seen. However a drop in wall temperature at the end of the insulated section can be seen for the low velocity case, but it does not affect the thermowell temperature in any significant manner. Insulating a short section of the pipe would be adequate to obtain accurate measurements of the gas temperature.

In all cases the bottom of the thermowell was seen to be at the gas temperature and was not affected by the changes in ambient conditions. A temperature measurement taken at the bottom of the thermowell therefore represented the temperature of the gas inside the pipe.

The CFD modelling was based on the following conditions:

- Pipe sizes between 8" and 24"
- Five ambient temperatures from -10 to 35 °C
- Gas temperatures of 15 and 37.7 °C
- Gas velocities down to 1.1 m/s

It should be noted that outside these conditions thermal lagging around the thermowell only is advisable. Also, only one design of thermowell was used in the CFD modelling and other thermowell designs may have different thermal characteristics.

### 5.3 Comparison between Experimental Measurements and CFD Modelling Calculations

The experimental measurements and the *CFD* Modelling show remarkable similarities.

- The *CFD* models all indicate that the temperature at the bottom of the thermowell is the same as the gas temperature both with and without insulation. The experimental measurements of Pallan confirm that the temperature in an unlagged thermowell was relatively insensitive to the most extreme ambient conditions.

- The *CFD* model shows that the temperature within the thermowell stabbing is influenced by ambient conditions but the temperature of the gas stream within the

pipe diameter is unaffected. This is confirmed by the experimental measurements of Nisbert and Robertson.

- The CFD model shows that the gas velocity within the thermowell stabbing is very low. In support of this, Ingram's temperature measurements within the thermowell stabbing showed that there was a very long response time to temperature changes.

- The *CFD* model shows that the temperature of the pipe wall is always very similar to the gas temperature. However, with insulation, the difference between the temperature of the pipe wall and the gas temperature is not detectable. Ingram confirmed that an insulated surface temperature measurement was within 0.1 ºC of the temperature in the thermowell.

- The *CFD* model shows that local insulation around a thermowell or a surface-mounted sensor is sufficient. There is no need to insulate the entire meter run. Ingram also confirmed that local insulation is sufficient for accurate measurements of gas temperature.

## 6 ACKNOWLEDGEMENTS

This work was sponsored by *Advantica*, *National Grid UKT*, *National Grid UKD*, *Scotia Gas Networks*, *Wales and West Utilities* and *United Utilities*. The authors would also like to thank Professor Malalasekera of *Loughborough University* for his CFD contributions.

## 7 REFERENCES

1 *Gas Meter Installations For Pressures Not Exceeding 100 Bar* The Institution of Gas Engineers Gas Measurement Procedures IGE/GM/1 Edition 2. **1998**

2 ISO 5167 *Measurement of fluid flow by means of pressure differential devices. Part 1. Orifice plates, nozzles and Venturi tubes inserted in circular cross-section conduits running full.* **1991**

3 ISO 5167 *Measurement of fluid flow by means of pressure differential devices. Part 1. Orifice plates, nozzles and Venturi tubes inserted in circular cross-section conduits running full.* **1997**

4 ISO 5167 Parts 1 and 2 *Measurement of fluid flow by means of pressure differential devices inserted in circular-cross section conduits running full*. **2003**

5 Pallan, W & Wood, KR *Thermowell Fatigue Failure Investigation* Gas Council Engineering Research Station Report ERS R247. April **1972**

6 Pallan, W Gas *Temperature Inferred from Pipe Wall Temperature* British Gas Engineering Research Station Report ERS R715 June **1974**

7 Fenwick, JS Pipe *Surface Temperature Measurement at Compressor Stations* British Gas Engineering Research Station Report ERS R1318. July **1976**

8 Ingram, R *Surface Temperature Transducer Response Time Tests on a St Fergus Gas Compressor* British Gas Engineering Research Station Report ERS R3995 July **1988**

9 Ingram, R *Effects of Removing Thermal Insulation on Surface Temperature Measurement – St Fergus* British Gas Engineering Research Station Report ERS R3996.April **1989**

10 Ingram, R *St Fergus Aftercooler Temperature Measurement* British Gas Internal Memorandum June **1986**

11 Nisbet, JR & Robertson, IC *Assessment of Gas Temperature Measurement Systems at Churchover Compressor Station* British Gas Engineering Research Station Report ERS R3670. April **1987**

12 Malalasekera, W *An Analysis of Heat Transfer in Thermowell Installations in Gas Pipelines* Wolfson School of Mechanical and Manufacturing Engineering, Loughborough University. August **2007**

13 Versteeg, HK & Malalasekera W, *An Introduction to Computational Fluid Dynamics: The Finite Volume Method* Second Edition. Pearson Education Ltd, **2007**